NAVAL POSTGRADUATE SCHOOL
Monterey, California

THESIS

THE DESIGN AND ANALYSIS OF A PHASED ARRAY MICROSTRIP ANTENNA FOR A LOW EARTH ORBIT COMMUNICATION SATELLITE
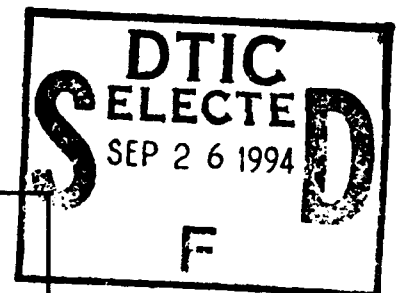
by

William Lee Barfield

June 1994

Thesis Advisor: Richard Adler

Approved for public release; distribution is unlimi' l.

94 9 23   079

1. AGENCY USE ONLY (Leave blank)	2. REPORT DATE June 1994	3. REPORT TYPE AND DATES COVERED Master's Thesis

4. TITLE AND SUBTITLE
THE DESIGN AND ANALYSIS OF A PHASED ARRAY MICROSTRIP ANTENNA FOR A LOW EARTH ORBIT COMMUNICATION SATELLITE

5. FUNDING NUMBERS

6. AUTHOR(S)
Barfield, William L.

7. PERFORMING ORGANIZATION NAME(S) AND ADDRESS(ES)
Naval Postgraduate School
Monterey, CA 93943-5000

8. PERFORMING ORGANIZATION REPORT NUMBER

9. SPONSORING / MONITORING AGENCY NAME(S) AND ADDRESS(ES)

10. SPONSORING / MONITORING AGENCY REPORT NUMBER

11. SUPPLEMENTARY NOTES
The views expressed in this thesis are those of the author and do not reflect the official policy or position of the Department of Defense or the U.S. Government.

12a. DISTRIBUTION / AVAILABILITY STATEMENT

Approved for public release; distribution is unlimited.

12b. DISTRIBUTION CODE

13. ABSTRACT (Maximum 200 words)

A Naval Postgraduate School spacecraft design class proposed a multiple beam, phased array, microstrip antenna as part of the preliminary design of a low earth orbit communication satellite. The antenna must provide coverage over the satellite's entire field of view while both uplink and down-link operate simultaneously on the same L-band frequency.

This thesis assesses the feasibility of the antenna proposed in that preliminary design. Design tradeoffs for a microstrip array constrained by both available surface area and a limited mass budget are examined. Two different substrate materials are considered in terms of weight and performance. Microstrip patch theory is applied to array element design and layout and antenna array theory is applied to determine phase and amplitude coefficients. The focus of the design is on obtaining the desired beam shape and orientation, given antenna size constraints. A corporate feed method is discussed and a general design presented.

Antenna performance is predicted through the use of a computer model based on Modal Expansion theory and results are plotted in a series of graphs which demonstrate the limitations of the proposed design.

DTIC QUALITY INSPECTED 3

14. SUBJECT TERMS
Microstrip Antenna, Low Earth Orbit Communication, Modal Expansion Theory, L-band, Satellite

15. NUMBER OF PAGES 96

16. PRICE CODE

17. SECURITY CLASSIFICATION OF REPORT Unclassified	18. SECURITY CLASSIFICATION OF THIS PAGE Unclassified	19. SECURITY CLASSIFICATION OF ABSTRACT Unclassified	20. LIMITATION OF ABSTRACT UL

. . .

**THE DESIGN AND ANALYSIS OF A PHASED ARRAY MICROSTRIP
ANTENNA FOR A LOW EARTH ORBIT COMMUNICATION SATELLITE**

by

William Lee Barfield
Lieutenant, United States Naval Reserve
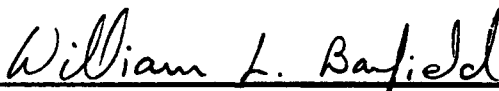B.S., North Carolina State University, 1984

Submitted in partial fulfillment
of the requirements for the degree of

MASTER OF SCIENCE IN ELECTRICAL ENGINEERING

from the

NAVAL POSTGRADUATE SCHOOL
June 1994

Author: _William L. Barfield_____
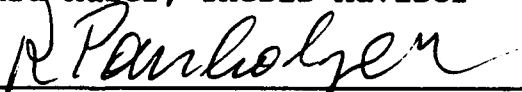   William Lee Barfield

Approved by: _RWA_____
             Richard Adler, Thesis Advisor

             _R Panholzer_____
             Rudolph Panholzer, Second Advisor

             _Michael C. Morgan_____
             Michael A. Morgan, Chairman
Department of Electrical and Computer Engineering

ii

ABSTRACT

A Naval Postgraduate School spacecraft design class proposed a multiple beam, phased array, microstrip antenna as part of the preliminary design of a low earth orbit communication satellite. The antenna must provide coverage over the satellite's entire field of view while both uplink and downlink operate simultaneously on the same L-band frequency.

This thesis assesses the feasibility of the antenna proposed in that preliminary design. Design tradeoffs for a microstrip array constrained by both available surface area and a limited mass budget are examined. Two different substrate materials are considered in terms of weight and performance. Microstrip patch theory is applied to array element design and layout and antenna array theory is applied to determine phase and amplitude coefficients. The focus of the design is on obtaining the desired beam shape and orientation, given antenna size constraints. A corporate feed method is discussed and a general design presented.

Antenna performance is predicted through the use of a computer model based on Modal Expansion theory and results are plotted in a series of graphs which demonstrate the limitations of the proposed design.

iii

Accesion For		
NTIS CRA&I	☑	
DTIC TAB	☐	
Unannounced	☐	
Justification		
By		
Distribution /		
Availability Codes		
Dist	Avail and / or Special	
A-1		

TABLE OF CONTENTS

LIST OF TABLES

LIST OF FIGURES

I. INTRODUCTION

A. BACKGROUND

In June 1991, Loral Cellular Systems Corporation of Palo Alto, California submitted a license request to the Federal Communications Commission for authority to build a world-wide, mobile communications system [Ref. 1]. Their proposed system, called GLOBALSTAR, is a satellite system designed to provide Radio-Determination Satellite Services (RDSS) for real time position location and tracking, as well as voice and data services. The system is intended to be integrated into the existing Public Switched Telephone Network (PSTN) and private cellular networks in order to provide telephone communications to users anywhere in the world.

In a project sponsored by the NASA/Universities Space Research Association Advanced Design Program, students at the Naval Postgraduate School, Monterey, CA performed a preliminary design [Ref. 2] for a satellite system based on the proposed GLOBALSTAR system. The focus of this thesis is on the design and performance analysis of a phased array L-band antenna, composed of microstrip patches, which was proposed as part of this preliminary design. The scope is limited to the design of the antenna panels and microstrip patches and to the performance analysis of overall antenna. While the beam

1

forming network will be mentioned, a detailed analysis of the beam forming network is outside the scope of this thesis. Similarly, certain mechanical details such as panel hinging and antenna deployment mechanisms as well as specific fabrication methods will not be considered in detail.

B. SYSTEM CONCEPT

Using this system, a mobile telephone user will have access to world wide coverage by accessing the PSTN via satellite. Using a special mobile telephone unit, a user communicates directly with a satellite via an L-band radio link. The satellite receives signals from mobile users and retransmits these signals to an earth based gateway via an S-band trunk link. In the reverse process, signals from the gateways are received by the satellite via the S-band link and then retransmitted to mobile users via the L-band link. Gateways are distributed across the globe and are connected to the PSTN.

Acquisition, synchronization, and satellite beam hand off coordination is provided for the gateways by a Satellite Operation Control Center (SOCC) as depicted in Figure 1.1. The information provided by the SOCC allows each gateway station to track and communicate with the satellites in its field of view. Ephemeris data is provided to the SOCC by several Tracking Telemetry and Control Stations (TT&C) which obtain the data through satellite observations. Overall

2

communications network management is provided by a Network
Control Center (NCC).
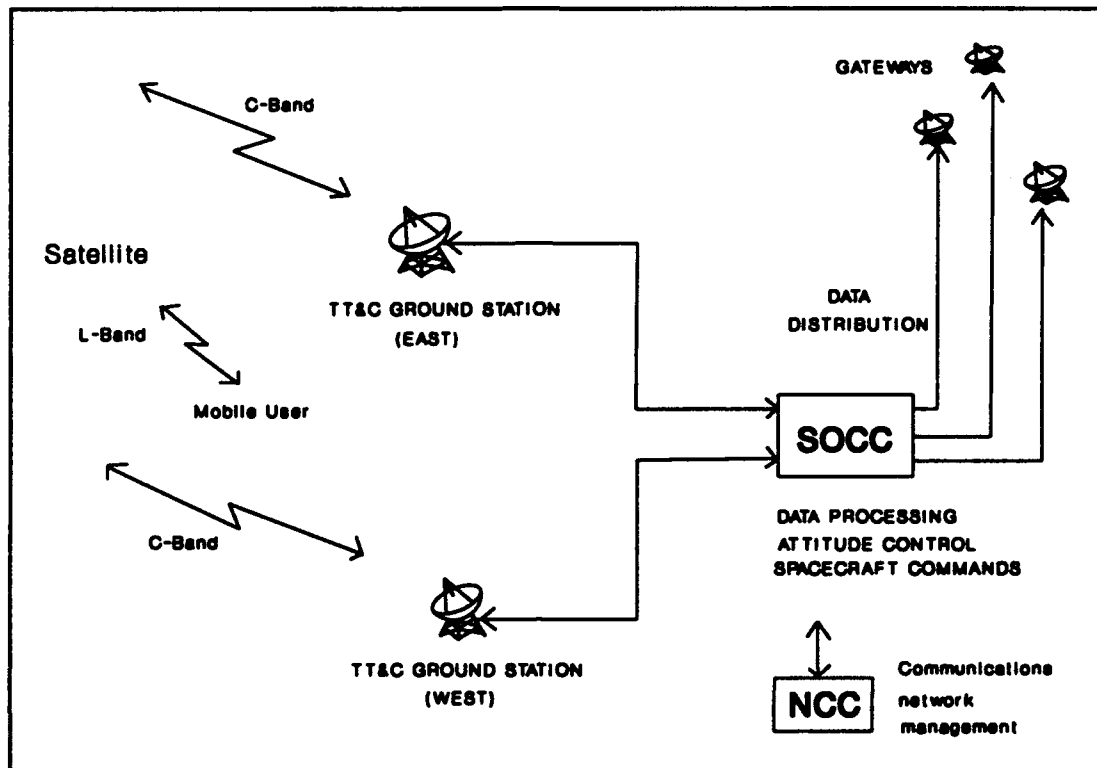
Figure 1.1 System Architecture

C. SYSTEM DESIGN

An orbital altitude of 750 nm gives a satellite field of
view of approximately 108 degrees (assuming a minimum
elevation angle of 10 degrees for the satellite observer).
This allows a constellation of 48 identical satellites in
circular orbits to provide continuous coverage between 75
degrees North latitude and 75 degrees South latitude.

The constellation is divided into eight orbital planes at an interval of 30 degrees with six satellites in each plane. There is no provision for on-orbit spares. Communication between the satellite and gateways is accomplished via an uplink and downlink at center frequencies of 6533.25 MHz and 5207.75 MHz respectively, each with a bandwidth of 16.5 MHz. A mobile user communicates with a satellite via an L-band link operating at a center frequency of 1618.25 MHz and a bandwidth of 16.5 MHz. A summary of the link budget as specified by [Ref. 1] is contained in Appendix A.

Each satellite provides communications coverage over its entire field of view through the use of six non-overlapping elliptically shaped spot beams. To maximize the amount of time a mobile user is illuminated by any one particular beam, beams are oriented such that their major axes are parallel to the spacecraft velocity vector. Figure 1.2 shows a typical coverage pattern for one satellite.

In order to minimize interference between channels, the six beams operate in pairs such that maximum beam separation is achieved on the ground. This is accomplished by switching beams on and off in pairs so that opposite pairs are active for 10 ms out of a 60 ms duty cycle. During the duty cycle, beam pairs alternate between transmit and receive functions.

SATELLITE

15° FOV CONTOUR

GROUND TRACK
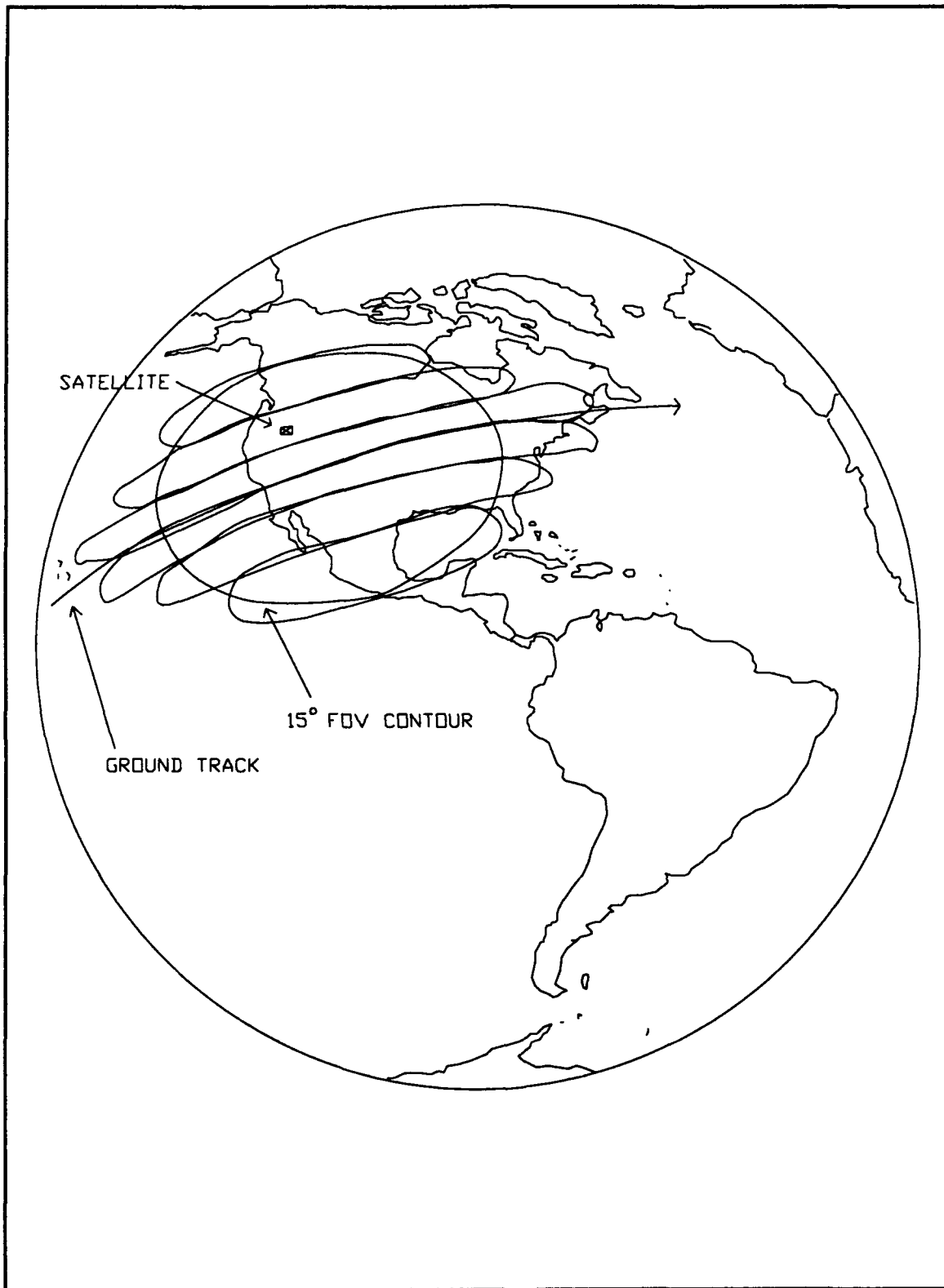
Figure 1.2. L-Band Beam Orientation

D. ANTENNA PERFORMANCE REQUIREMENTS

The L-band antenna for this system must not only provide adequate gain, but must also correctly shape each of the six spot beams while maintaining low sidelobes. The antenna must also allow the communications payload to maintain a constant bit error rate (BER). Bit error rate is a function of carrier to noise ratio (C/N) and C/N is a function of path length. Because antenna beams must be statically scanned off center to cover the FOV, the path length for each of the six antenna beams is different. Path lengths vary from a minimum of 1748 km (measured along antenna boresight) for the inner most beams, to a maximum of 9066 km for the outer most beams. In order to maintain a constant BER, an isoflux antenna is required. Table I-1 summarizes the L-band antenna performance parameters.

TABLE I-1. ANTENNA PARAMETERS

f_0=1618.25 BW=16.5 (MHz)	Beam 1 & 6	Beam 2 & 5	Beam 3 & 4
Center	45°	30°	10°
BW (-4 dB)	25° × 110°	35° × 120°	40° × 120°
BW (total)	40° × 120°	50° × 120°	70° × 140°
Gain (dBi)	6.5	5.5	4.0

Note: Satellite FOV is 108°

6

II. DESIGN CONSIDERATIONS

A. SPACECRAFT CONFIGURATION

1. Overview

The spacecraft is designed to be placed into orbit using the Delta 7925 launch vehicle. A Satellite Launch Dispenser (SLD) was designed so that a single launch vehicle can place an entire plane of satellites into orbit at one time. The SLD is essentially a chest of drawers where the spacecraft are the drawers. The spacecraft slide into the SLD along rails and compress a spring when properly seated. Each spacecraft is then held in place by explosive bolts. At the appropriate time during orbit insertion, the explosive bolts are fired and a spacecraft is ejected into the proper orbit.

2. Size Constraints

The Delta payload shroud and the SLD impose serious size constraints on overall spacecraft size. In order to fit into the space provided by the SLD, the spacecraft dimensions can not exceed 1.4 x 1.4 x 0.6 meters. The space allowed for the L-band antenna alone is 1.4 x 1.4 x 0.1 meters in the stowed configuration. The preliminary design allowed an antenna mass budget of 10 kg however this proves to be unrealistic.

B. ANTENNA CONFIGURATION

In order to achieve beam steering and beam shaping characteristics necessary to meet the antenna performance requirements, a planar phased array antenna similar to the L-band antenna of [Ref. 3] was considered. A planar array allows both beam shaping and beam steering in any direction. For simplicity, rectangular microstrip patch array elements were chosen. A microstrip antenna is both lightweight and easily fabricated using common printed circuit board etching techniques [Ref. 4]. Disadvantages usually associated with microstrip antennas, specifically large surface area require- ments and narrow bandwidth [Ref. 5], were found to be insigni- ficant in this application. Folding array panels are employed so that the antenna can be stowed in the space available and conveniently deployed via a spring-loaded mechanism once the spacecraft is in the proper orbit. Each array panel corresponds to one of the six antennas necessary to form the appropriate beam. Figure 2.1 shows the phased array antenna in the deployed configuration.

C. MICROSTRIP PATCH THEORY

The simplest and most common type of microstrip antenna is the rectangular patch mounted on a dielectric substrate of thickness h, shown in Figure 2.2.
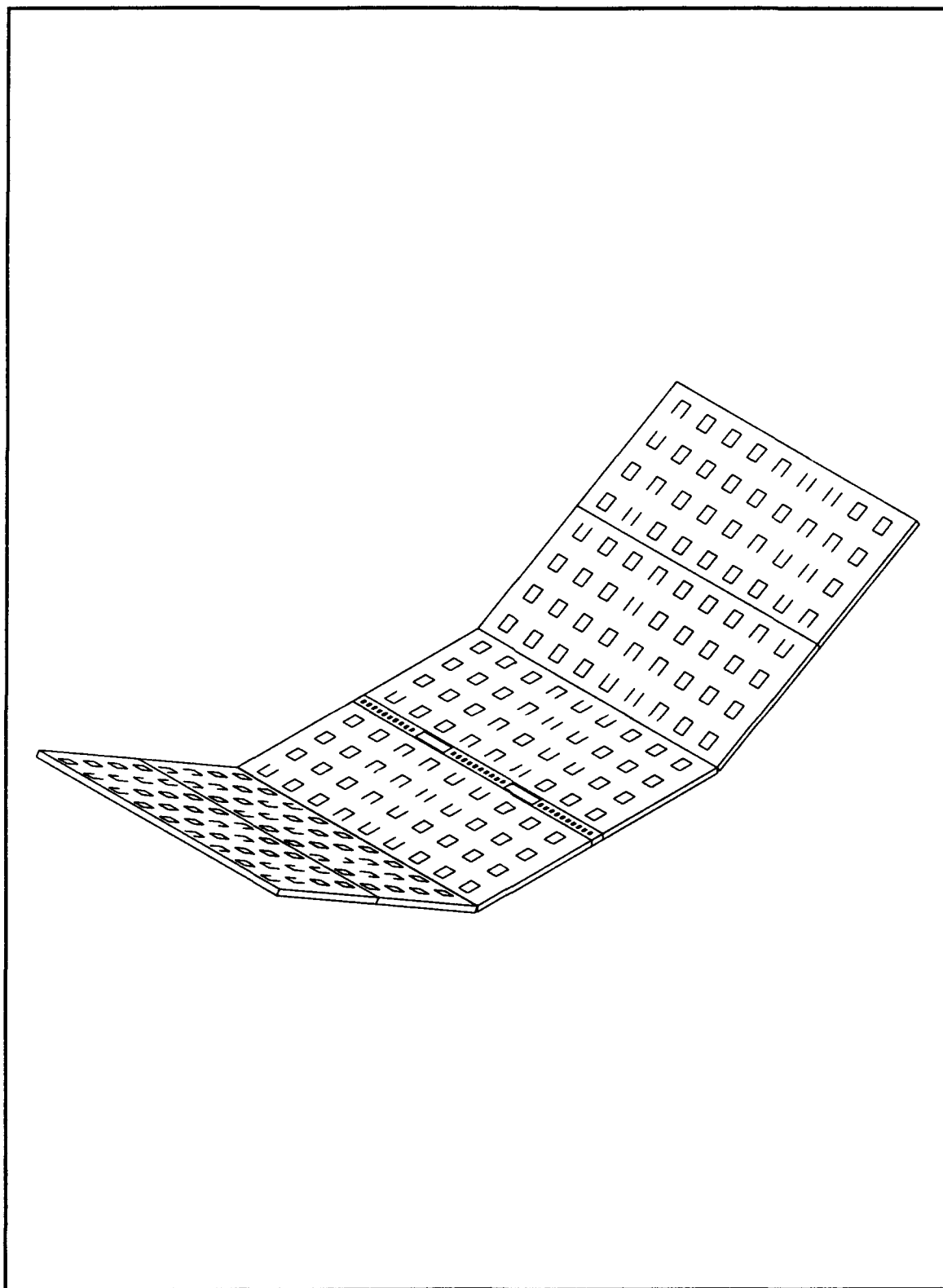
Figure 2.1.   Phased Array Antenna

COPPER PATCH

DIELECTRIC
SUBSTRATE

FEED POINT

L

W

h

GROUND PLANE
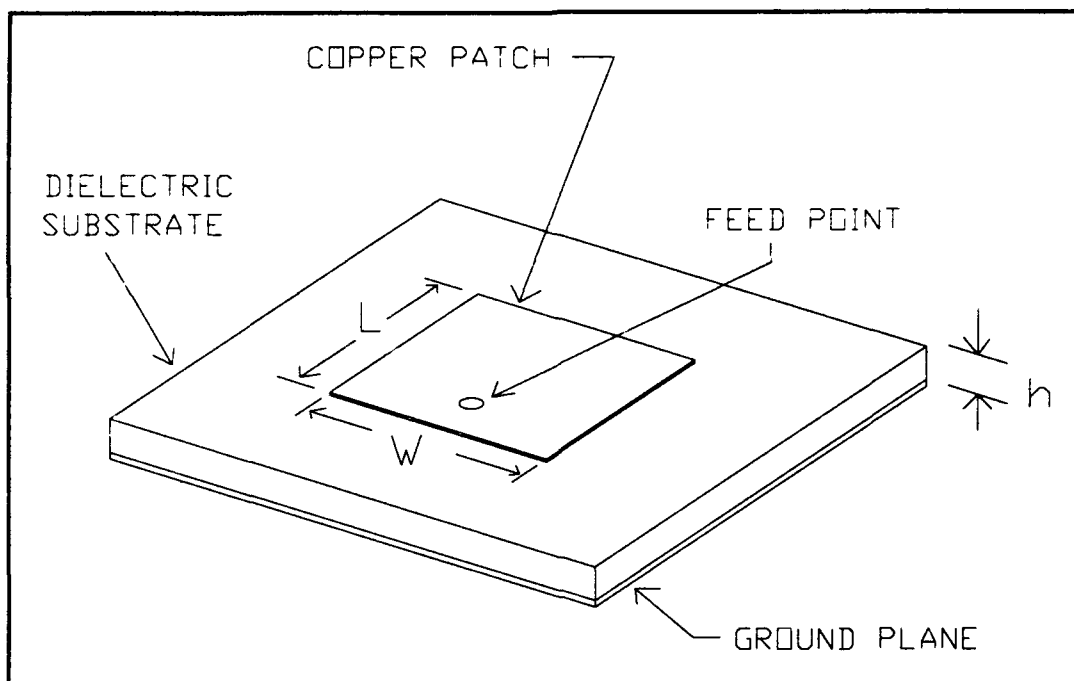
Figure 2.2. Rectangular Microstrip Patch

1. Radiation Mechanisms

The radiation mechanism of a microstrip patch can be modeled in one of several ways, each with its advantages and disadvantages.

a. The Wire Grid Model

A microstrip patch can be modeled as a grid of fine wires [Ref. 6]. The currents on the wires are solved for numerically and when found, provide accurate information about the antenna pattern and input impedance. The disadvantage of this method is that it requires an extraordinary amount of computer resource [Ref. 7].

10

b. The Modal Expansion Model

The modal expansion model, which is valid for electrically thin (h«λ) substrates, represents the antenna as a thin TM mode cavity bounded by magnetic walls [Ref. 5] within which the dominant TM mode is excited along with other non-resonant modes. As long as the dominant mode is sufficiently excited, this model provides accurate performance information [Ref. 7], including the effects of feed location. The ability to account for a feed probe and handle complex patch shapes are the chief advantages of this model.

c. The Transmission Line Model

The transmission line model considers the patch to be a line resonator with radiation due to fringing fields at the open circuited ends [Ref. 6]. The radiator consists of two radiating slots separated by a distance L. The slots are formed at the edges of the patch element, between the patch and the ground plane below. Field variations along the radiating edges are ignored. The chief disadvantage of the transmission line model is that it is only valid for rectangular patches. The input impedance of the transmission line model is also highly dependent on feed location and fails to accurately predict input impedance for all feed locations [Ref. 7]. However, formulas have been developed to predict input impedance for any feed location [Ref. 6].

Despite its drawbacks, the transmission line model's main advantage is, that for rectangular patches, it

provides simple design formulas which give reasonably accurate performance predictions.

2. Patch Parameters

The dimensions of a rectangular patch, as well as bandwidth and gain, are determined by the operating frequency of the antenna, the relative dielectric constant, and thickness of the substrate material. The following formulas are based on the transmission line model.

a. Width and Length

The width and length of a rectangular microstrip patch are given by:

$$W = \frac{c}{2f_r}\left[\frac{\varepsilon_r + 1}{2}\right]^{-\frac{1}{2}} \quad (cm) \qquad (2.1)$$

$$L = \frac{c}{2f_r\sqrt{\varepsilon_e}} - 2\Delta l \quad (cm) \qquad (2.2)$$

where

c = speed of light (m/s),

f_r = operating frequency (MHz),

ε_r = relative dielectric constant,

ε_e = effective dielectric constant,

$$\varepsilon_e = \frac{\varepsilon_r + 1}{2} + \frac{\varepsilon_r - 1}{2}\left(1 + \frac{12h}{W}\right)^{-\frac{1}{2}} , \qquad (2.3)$$

12

$$\Delta l = 0.412h \ \frac{(\varepsilon_e + 0.3) \ (\frac{W}{h} + 0.264)}{(\varepsilon_e - 0.258) \ (\frac{W}{h} + 0.8)} \qquad (2.4)$$

and

h = dielectric thickness (cm) [Ref. 6].

b. Bandwidth

The bandwidth of a microstrip antenna is defined in terms of the antenna's quality factor (Q) as follows:

$$BW = \frac{VSWR - 1}{Q\sqrt{VSWR}} \qquad (2.5)$$

Where VSWR is less than a specified value (2:1 or 1.5:1 for example) and VSWR=1 at the operating frequency [Refs. 5 and 6], the bandwidth is dependent on both the relative dielectric constant, ε_r, and thickness of the substrate. Thicker substrates and lower values of ε_r give larger bandwidths. Typically, microstrip antennas have bandwidths on the order of a few percent of the operating frequency.

c. Gain

Gain is also affected by substrate thickness and relative dielectric constant. Gain is inversely proportional to ε_r and directly proportional to substrate thickness. To achieve the necessary gain, microstrip patches can be arranged to form linear and planar arrays.

D. ARRAYS

The radiation pattern of a single array element is relatively wide and typically has low gain. In order to achieve higher directivity and additional gain, antenna elements can be arranged to form linear or planar arrays.

1. Theory

The total field of an array is given by the vector addition of the fields radiated by individual elements [Ref. 8]. The required directivity is achieved by arranging individual element excitations such that fields produced by each element interfere constructively in the desired direction and interfere destructively in all other directions. The radiation pattern of an array is obtained by multiplying the field produced by a single element by an array factor (AF). The array factor for an array of N identical elements is given by [Ref. 8] as

$$AF = \sum_{n=1}^{N} I_n e^{j(n-1)\psi} \qquad (2.6)$$

where

N = number of elements,

I_n = element excitation coefficient,

$$\psi = kd \times \cos(\theta) + \beta , \qquad\qquad (2.7)$$

and

k = wave number,

d = distance between elements (m),

θ = direction of main beam (degrees),

β = phase shift between elements (degrees) [Ref. 8].

The main beam can be scanned in any direction by adjusting the progressive phase shift between elements.

M arrays of N elements can be arranged to form a planar array which will allow the beam to be scanned in any direction. Additionally, array elements can be excited non-uniformly to control the beam shape. If a coordinate system such as that of Figure 2.3 is chosen, it is shown in [Ref. 8] that the array factor in the X direction is given by

$$AF_x = \sum_{m=1}^{M} I_{m1} e^{j(m-1)(kd_x \sin(\theta)\cos(\phi) + \beta_x)} \qquad\qquad (2.8)$$

Similarly, the array factor in the Y direction is given by

$$AF_y = \sum_{n=1}^{N} I_{1n} e^{j(n-1)(kd_y \sin(\theta)\sin(\phi) + \beta_y)} , \qquad\qquad (2.9)$$

where

I_{m_1} = excitation coefficient for m elements and

I_{1_n} = excitation coefficient for n elements.
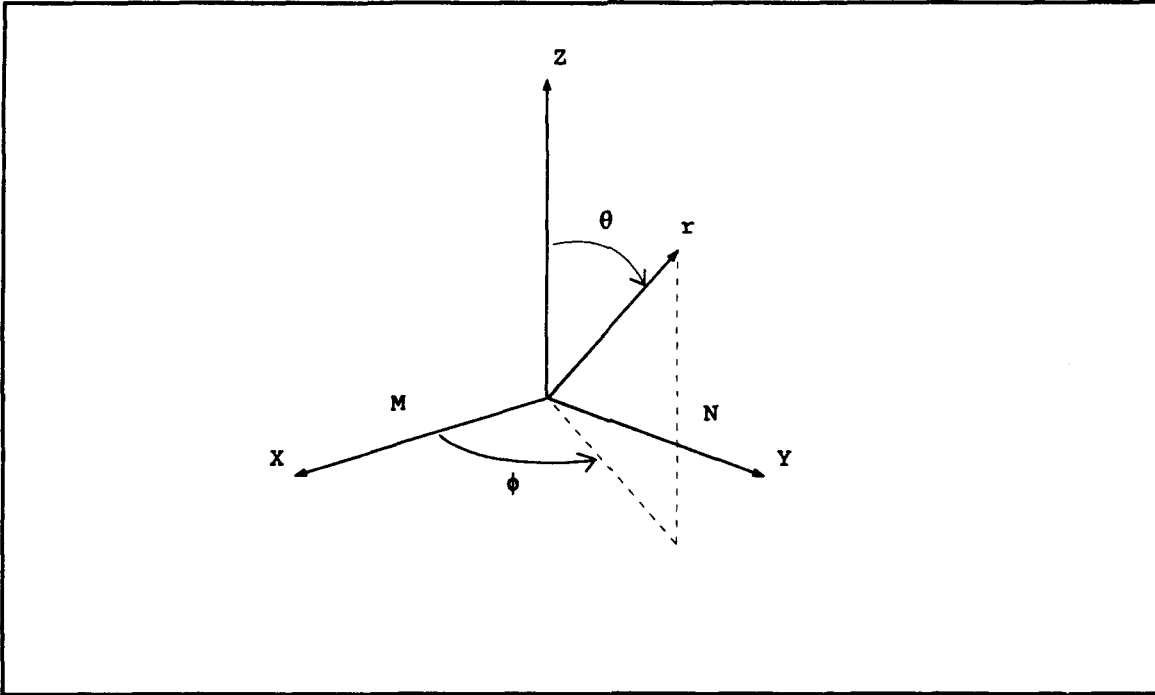
Figure 2.3. Array Coordinate System

The total array factor is the product of AF_x and AF_y and is given by

$$AF = \sum_{m=1}^{M} I_{m1} e^{j(m-1)(kd_x \sin(\theta)\cos(\phi) + \beta_x)} \sum_{n=1}^{N} I_{1n} e^{j(n-1)(kd_y \sin(\theta)\sin(\phi) + \beta_y)}$$

(2.10)

2. Beam Synthesis

The beam in a phased array antenna is shaped by non-uniform excitation of the array elements. This non-uniformity can be in amplitude, phase, or both. Using general synthesis [Ref. 9] and optimization [Refs. 10 and 11] techniques, beams of almost any shape and contour can be formed. For less

stringent beam shape criteria, a simpler synthesis method based on the Fourier transform method presented in [Ref. 8] has been derived.

In the Fourier transform method, excitation coefficients are related to the Fourier transform of the array factor expressed as a function of ψ, which is itself a function of θ and ϕ. Excitation coefficients are given by

$$I_n = \frac{1}{2\pi} \int_{-\pi}^{\pi} AF(\psi) \, e^{jn\psi} \, d\psi \quad ,$$

$$-N \le n \le N$$

(2.11)

for an odd number of elements, and

$$I_m = \frac{1}{2\pi} \int_{-\pi}^{\pi} AF(\psi) \, e^{-j[\frac{(2m+1)}{2}]\psi} \, d\psi \quad ,$$

$$-M \le m \le -1$$

(2.12)

and

$$I_m = \frac{1}{2\pi} \int_{-\pi}^{\pi} AF(\psi) \, e^{-j[\frac{(2m-1)}{2}]\psi} \, d\psi \quad ,$$

$$1 \le m \le M$$

(2.13)

for an even number of elements [Ref. 8].

Equations 2.11 - 2.13 yield complex numbers which represent the amplitude and phase excitation of an element. The total excitation coefficient is obtained as the product of I_n and I_m.

III. ANTENNA DESIGN

A. MICROSTRIP PATCH DESIGN

1. Substrate Material

The first step in the design process is the selection of a dielectric substrate material. The dominant features of a microstrip array are controlled by substrate parameters such as thickness and permittivity more than by the particular element type [Ref. 12].

Because weight is a primary consideration in spacecraft design, a substrate must be chosen which not only has satisfactory dielectric properties, but which also has low density. There are a variety of substrate materials available with a wide range of relative dielectric constants and densities. Tables summarizing various materials and their relevant properties can be found in [Refs. 5 and 6].

Two representative substrate materials which were considered for this design are Duroid (RT 5870), produced by Rogers Corporation of Chandler, AZ, and Kevlar (HI 4093), produced by Arlon Electronic Substrates Division of Rancho Cucamonga, CA.

Studies have shown [Ref. 13] that efficiency and bandwidth are nearly independent of patch shape (i.e., circular vs rectangular) and are determined mainly by substrate thickness and permittivity.

18

In order to achieve good resolution in beam shape and steering, the number of array elements must be maximized within available array area and element spacing constraints. This is accomplished by making the microstrip patches as small as possible while maintaining acceptable performance characteristics. For a given operating frequency, patch size is determined by relative dielectric constant and substrate thickness. Figure 3.1 shows the effect of relative dielectric on patch width based on equation (2.1). Figure 3.2 shows the effect of dielectric thickness (h) on patch length for a given operating frequency and relative dielectric constant, based on equation (2.2).

Duroid substrates are available with ε_r ranging from 2.1 to 10.0. Higher ε_r yields a smaller patch size at the expense of bandwidth and gain. Rogers Duroid RT 5870 has ε_r equal to 2.23 which allows higher efficiency and bandwidth performance but the density of RT 5870 Duroid is 2.2 gm/cm^3. Arlon's HI 4093 Kevlar material on the other hand, has a relative dielectric constant of 3.9 and a density of 1.38 gm/cm^3.

For a given operating frequency and dielectric thickness, Kevlar yields a smaller patch size than Duroid and although efficiency and bandwidth performance are reduced, the results are still within acceptable parameters. Therefore, the lower mass of Kevlar far outweighs its disadvantages.
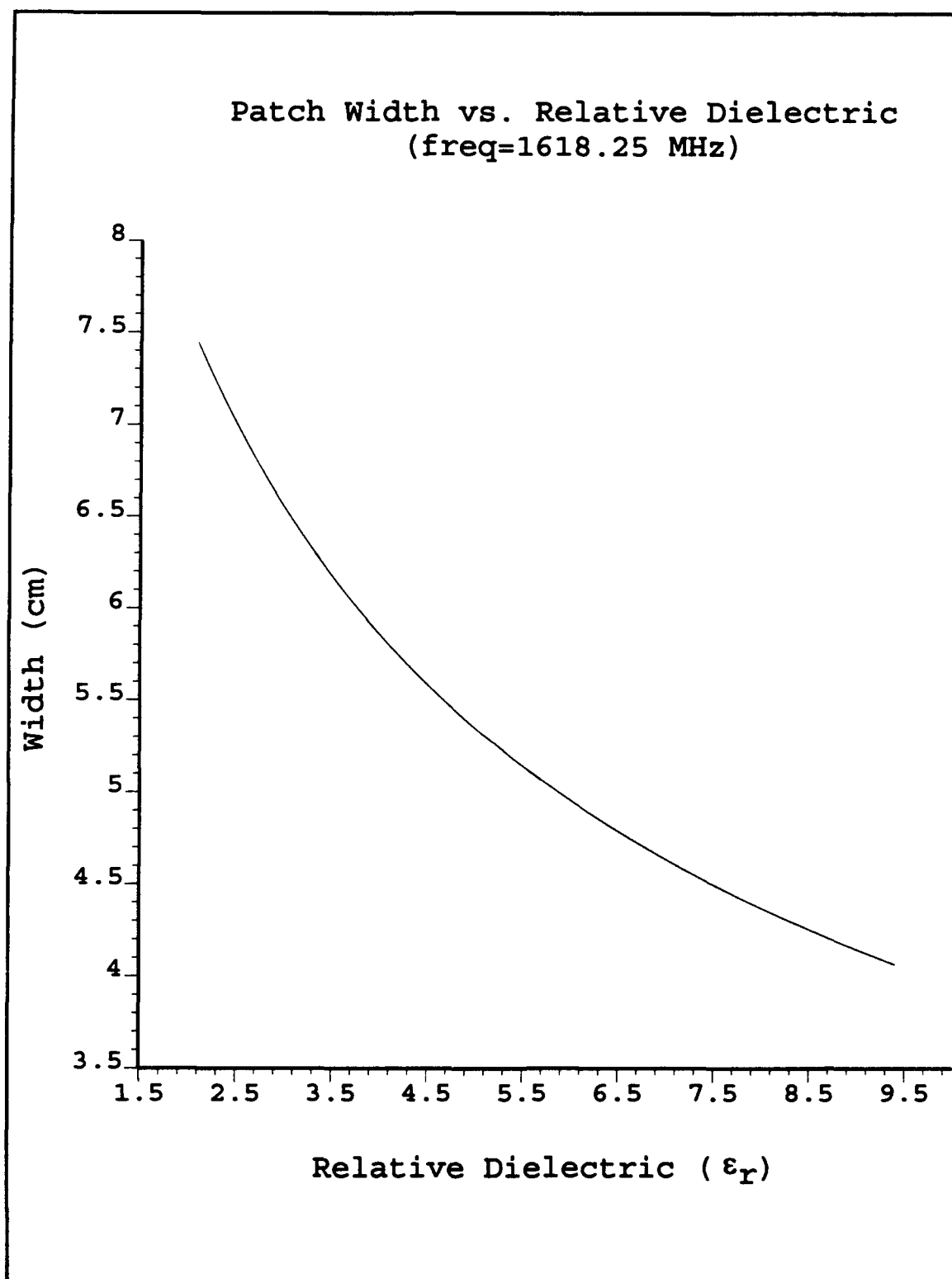
Figure 3.1. Effect of ε_r on Width of a Microstrip Patch
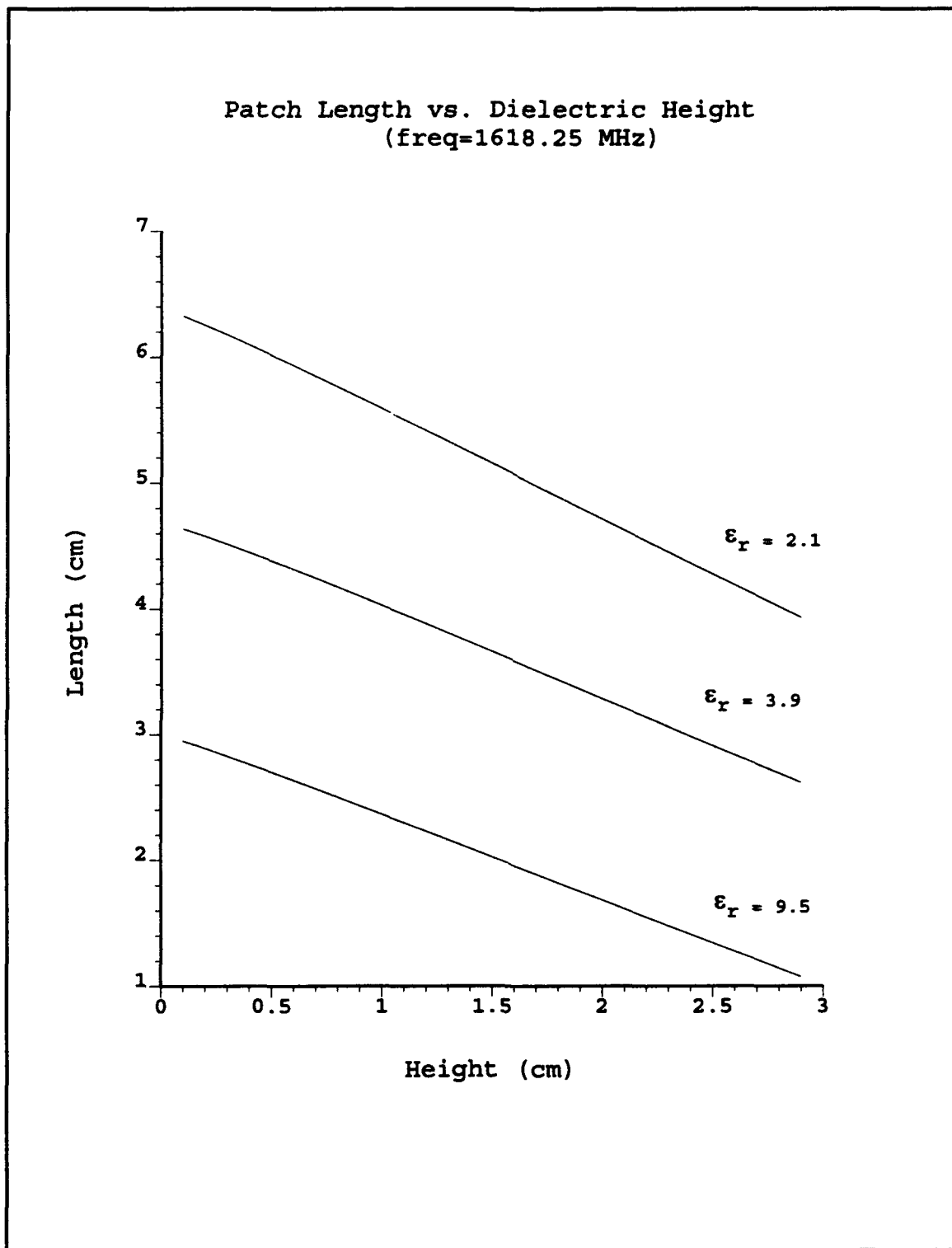
Figure 3.2. Effect of Height and ε_r on Length of a Microstrip Patch

Using a solid Duroid dielectric 0.3 cm thick, the mass of the substrate alone would be 36.7 kg (for an antenna area of 1.4 m × 4.0 m). A Kevlar substrate with the same dimensions would yield an antenna mass of 23.3 kg. Appendix B contains detailed mass estimates for antenna components.

2. Patch Dimensions

a. Thickness

Because the antenna substrate and ground plane must form the array panels, they must be made thick enough to provide the required rigidity. The array panels must be rigid enough to withstand structural loads of launch and deployment as well as resist warpage due to thermal cycling. A substrate thickness of at least 0.3 cm was selected and assumed adequate to meet these criteria. The antenna mass could be reduced without significantly affecting electrical and mechanical performance by supporting a thin dielectric substrate on a honey-comb structure such as that described in [Refs. 3 and 4]. The effect of raising the height of the patch above the ground plane is to increase bandwidth [Ref. 13], while reducing dielectric thickness would have the opposite effect.

b. Area

The equations presented in Chapter II can be used as a starting point for determining patch dimensions which can later be optimized using a more sophisticated model. For an operating frequency of f_r=1618.25 MHz and a relative dielectric constant ε_r=3.9, equations (2.1)-(2.4) yield a

patch length of 5.8 cm and a width of 7.2 cm (note that the width is defined as the long dimension of the rectangle). The gain of a single patch is approximately 5 dB. Detailed calculations for length, width, efficiency, directivity, and gain calculations for a single patch are contained in Appendix C.

A FORTRAN computer program which makes use of modal expansion theory was used in an iterative process to optimize the values for patch length given a constant width. A listing of the program is contained in Appendix F. The final values for length and width are summarized in Table III-1 along with the operating parameters for a single microstrip patch.

TABLE III-1. PARAMETERS FOR A SINGLE MICROSTRIP PATCH

ε_r=3.9, h=0.3 (cm) f_r=1618.25 MHz	L (cm)	W (cm)	G (dB)	% BW
Transmission Line	4.6	5.9	5.02	2.42
Modal Expansion	4.44	5.9	5.02	2.62

B. PLANAR ARRAY DESIGN

Six array panels are needed to produce the six elliptically shaped beams. The beams are symmetrical from outboard to inboard with beams 1 & 6 being identical, beams 2 & 5 identical, and beams 3 & 4 identical. The total area available for each array panel in the deployed configuration is 0.9338 m^2.

1. Element Spacing

As previously stated, the number of array elements needs to be maximized in order to achieve good beam resolution. At the same time, the array elements must be placed far enough apart to avoid mutual coupling which would degrade performance by increasing side lobe levels (SLL). It has been shown [Ref. 14] that for an element spacing of d > $\lambda/2$, mutual coupling will not cause significant side lobe levels. Measurements made on L-band microstrip arrays have shown that mutual coupling levels of -25 dB or less can be achieved with proper element spacing [Refs. 14 and 15]. If the elements are separated by much more than one half wavelength, unwanted grating lobes are produced. An element spacing of about 0.55λ has been shown to give good results [Ref. 3]. To avoid grating lobes and mutual coupling effects, the patch spacing for this design was chosen as 0.1017 m (0.55λ). This spacing allows a 4 × 9 element array to be placed on each of the six antenna panels.

2. Excitation Coefficients

The Fourier transform method which was previously developed for a planar array was used to obtain element phase and amplitude excitation coefficients. Array coefficients for a single beam are shown in Table III-2. The resulting array factors are plotted in Figure 3.3 and Figure 3.4. The excitation coefficients are tabulated in Appendix D and array factor plots for each beam are presented in Appendix E.

24

TABLE III-2. BEAM 1 EXCITATION COEFFICIENTS

Element Number	1	2	3	4
1	0.013 ∆52.36°	0.046 ∆-127.6°	0.046 ∆-127.6°	0.013 ∆52.36°
2	0.019 ∆-57.73°	0.066 ∆129.3°	0.066 ∆129.3°	0.019 ∆-57.73°
3	0.024 ∆-153.8°	0.083 ∆28.18°	0.083 ∆28.18°	0.024 ∆-153.8°
4	0.027 ∆103.1°	0.094 ∆-76.9°	0.094 ∆-76.9°	0.027 ∆103.1°
5	0.028 ∆0.0°	0.098 ∆180.0°	0.098 ∆-180.0°	0.028 ∆0.0°
6	0.027 ∆-103.1°	0.094 ∆76.9°	0.094 ∆76.9°	0.027 ∆-103.1°
7	0.024 ∆153.8°	0.083 ∆-28.18°	0.083 ∆-28.18°	0.024 ∆153.8°
8	0.019 ∆57.73°	0.066 ∆-129.3°	0.066 ∆-129.3°	0.019 ∆57.73°
9	0.013 ∆-52.36°	0.046 ∆127.6°	0.046 ∆127.6°	0.013 ∆-52.36°

3. Antenna Gain

The maximum array gain is the sum of individual element gains less losses associated with the array feed. The maximum gain is 20.6 dBi. This is well above the maximum required (6 dBi) for any antenna panel, however, a significant amount of loss will occur in the feed structure and must be offset by the excess gain.
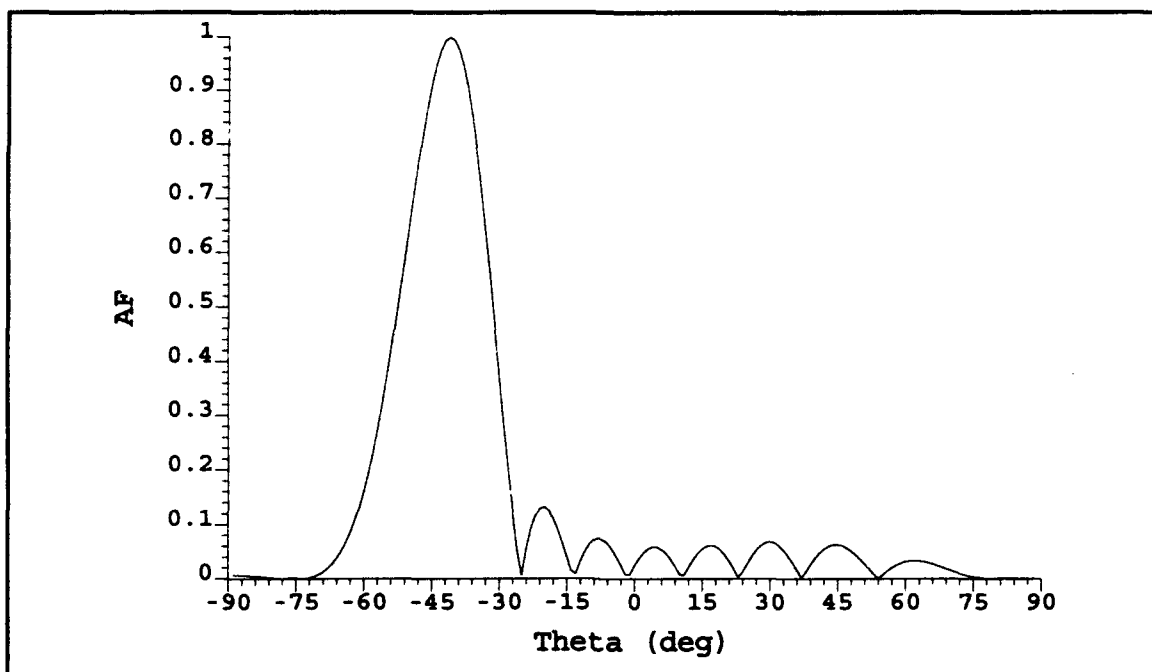
Figure 3.3. Beam 1 Array Factor ($\phi=90°$)
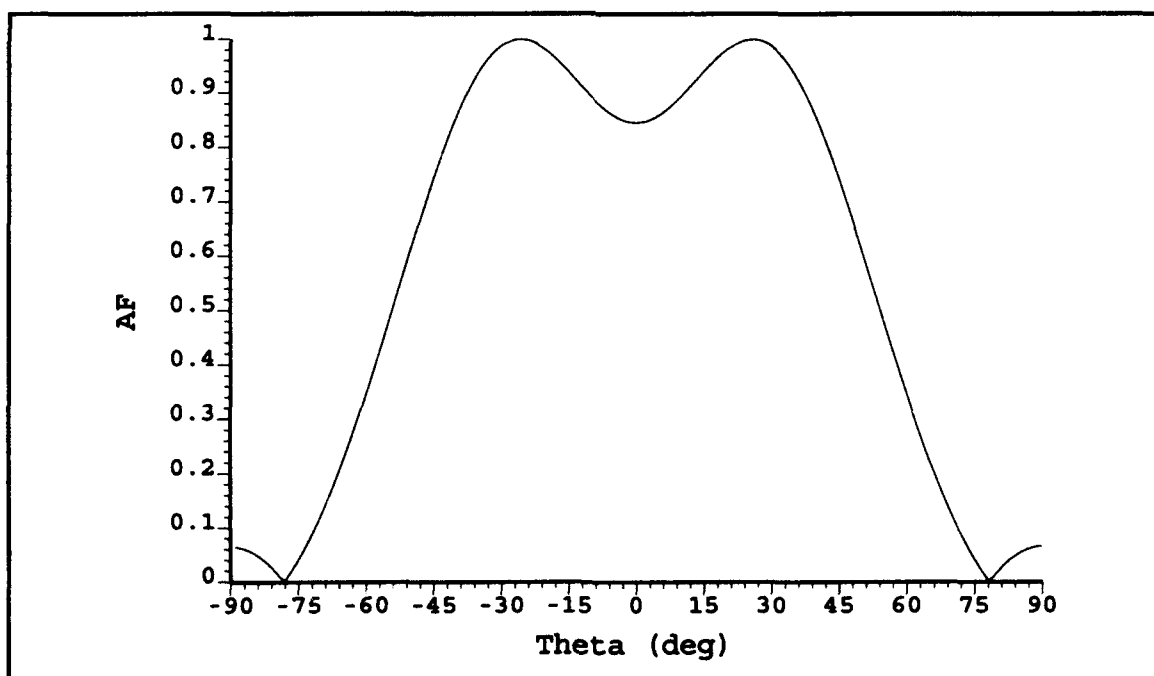
Figure 3.4. Beam 1 Array Factor ($\phi=0°$)

4. Feed Methods

There are a variety of feed methods for microstrip patch arrays and for each method there exists many variations. In general, feed methods are grouped into three categories - probe, corporate, and triplate feeds - and are briefly discussed next.

a. Probe Feed

In the probe feed method, each patch is connected to the feed network via a coaxial-fed probe which extends through the ground plane and substrate. The probe is physically attached to the patch by a solder joint. Impedance matching between the coax and array element can be accomplished for thick substrates by designing a teardrop-shaped probe which cancels out probe inductance [Ref. 3] or by varying the diameter of the probe for thin substrates [Ref. 16]. Obviously it would be impractical to construct an array where each element had its own coaxial feed cable. The weight and space requirements would be prohibitive for spacecraft applications.

b. Corporate Feed

A corporate feed offers a practical solution to the array feed problem by allowing one coaxial line to feed a network composed of microstrip transmission lines. A series of power dividers delivers power to and from the radiating elements. The microstrip transmission line provides equal path length to all elements maintaining phase between

elements. The two major disadvantages of the corporate feed
are that there is not enough room on a planar array substrate
for radiating elements and the feed network, and high line
loss occurs due to long path lengths. The second disadvantage
can be overcome by integrating active elements into the
substrate [Refs. 17 and 18] or by breaking the feed network
into subsections, each of which is fed by a low loss coaxial
cable [Ref. 19].

c. Triplate Feed

In a triplate feed (also called a hybrid feed),
the feed network is etched on its own substrate layer and
either laminated to the underside of the radiating element's
substrate or attached to the backside of the ground plane.
The former method requires the radiation of the feed network
to be accounted for in the antenna design while the latter
method eliminates feed radiation effects and divides the
design problem into two parts: the array itself and the feed
network.

(1) Feed Network in Front of Ground Plane. A
triplate feed located in front of the ground plane and
directly under the radiating element's substrate simplifies
the array construction at the expense of increased design
complexity. The metal pins used to attach the array element
to the feed network are eliminated through electromagnetic
coupling. Impedance matching is controlled by the amount of
overlap between the microstrip patch and the feed network.

Radiation effects can be largely reduced by locating the feed network as close to the ground plane as possible. [Ref. 13]

(2) Triplate Behind Ground Plane. If the corporate feed network is located behind the ground plane, radiation effects from the feed network are eliminated at the expense of a more complicated and expensive physical construction involving plated through holes and connecting pins.

5. Feed Design

Although antenna feed design is discussed in [Ref. 20], a complete design is outside the scope of this thesis. A brief discussion of a possible feed method is included to prove the feasibility of providing the required array element excitations.

A triplate corporate feed located behind the antenna ground plane could be used. This feed method, based on those presented in [Refs. 6 and 19], would simplify antenna performance analysis by eliminating feed radiation effects. Since the antenna is a statically scanned array, the required phase shifts and impedance matching could be built into the microstrip feed lines using microstrip transmission line techniques. Figure 3.5 shows one possible feed layout.

C. SUMMARY

An exploded view of one antenna panel is illustrated in Figure 3.6.
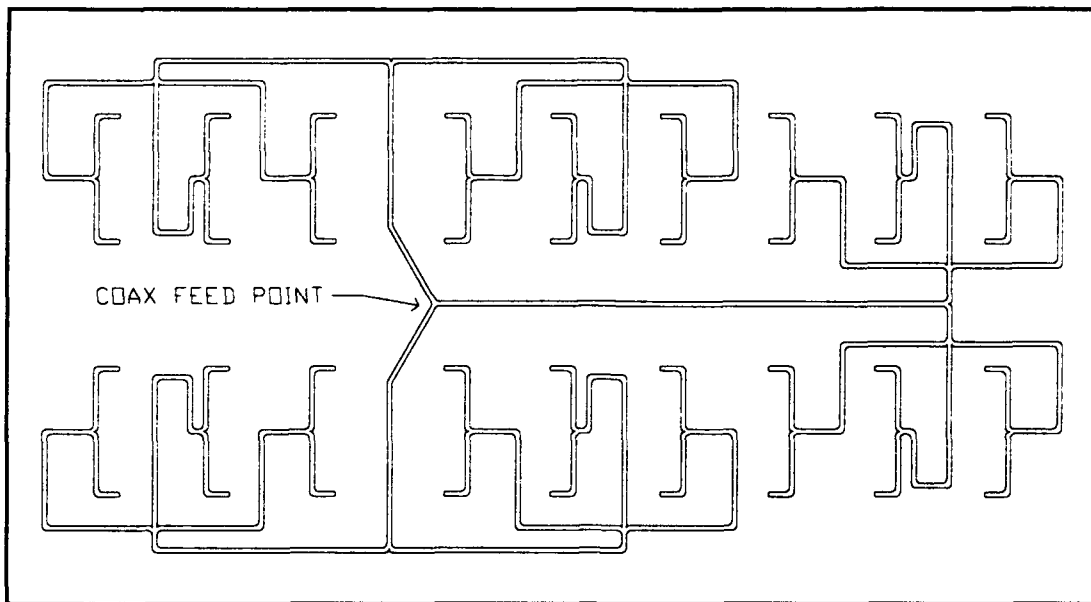
Figure 3.5. Coax Corporate Feed
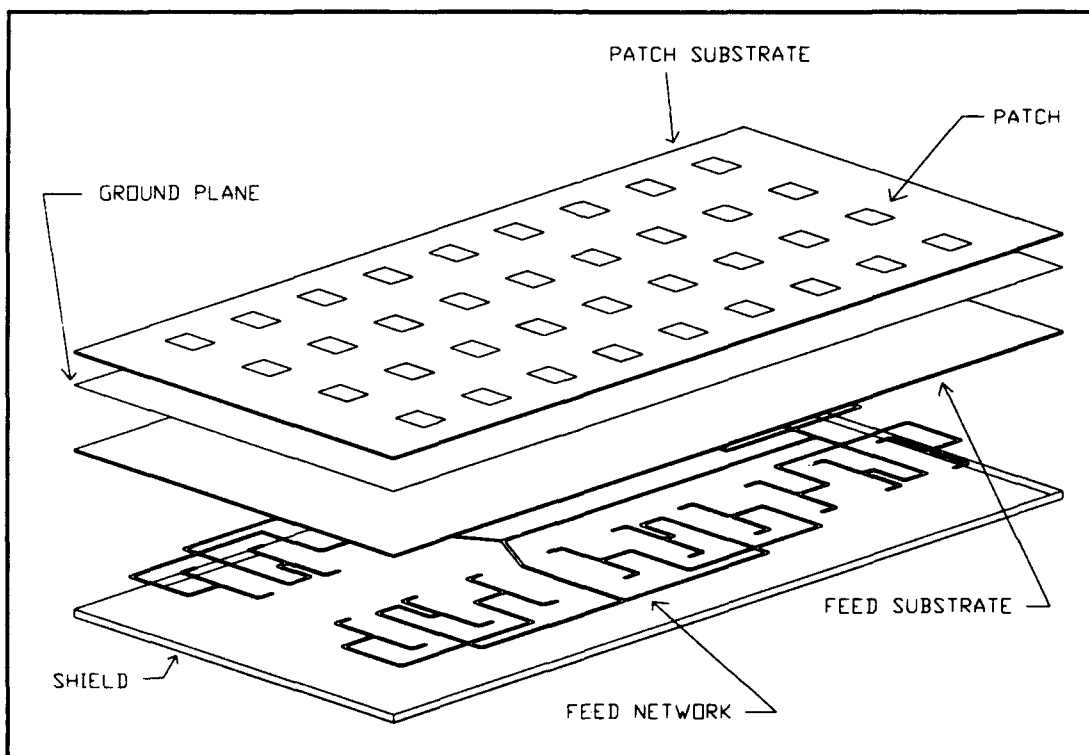
Figure 3.6. Antenna Panel Assembly

IV. PERFORMANCE ANALYSIS

A. ANTENNA MODEL

Chapter II described the wire grid, transmission line, and modal expansion models which are used to analyze and predict the performance of microstrip antennas. The wire grid model is unsuitable for use on any but the simplest of problems due to the computational resource required. Because the transmission line model and the modal expansion model do not account for surface waves in the dielectric substrate and do not account for mutual coupling, they do not provide the most accurate solution available [Ref. 16]. However, it will be shown that for arrays with proper element spacing, and all but extreme scan angles, the modal expansion modal provides adequate results with relative ease of computation. The areas where the modal expansion model fails will be discussed and shown to be insignificant for this analysis.

1. Infinite vs. Finite Arrays

The analysis of an infinite array yields adequate results for the inner array elements and accounts for a change in impedance with varying scan angle. Infinite array analysis ignores edge effects due to surface waves in the dielectric. The analysis of a finite array includes these edge effects but at the expense of more difficult calculations. It has been shown that surface wave power increases with dielectric

31

thickness and that for a thin dielectric ($h \leq 0.03\lambda$), surface wave power is negligible [Ref. 14]. It has also been shown that surface wave power diminishes with increasing array size and that for array sizes of 7 × 7 or greater an infinite approximation is acceptable [Ref. 21].

2. Edge Effects

Diffractions cause by the finite edge of the ground plane play a significant part in the radiation pattern at wide scan angles and in the backlobe region. The Geometric Theory of Diffraction (GTD) can be combined with other analysis methods to provide an accurate antenna performance model in these regions. Diffraction edge effects can be ignored for scan angles less than about 70° [Ref. 22].

3. Input Impedance

Although the modal expansion model enables calculation of input impedance, patch currents near the feed point are not modeled. This results in inaccurate impedance. It has been shown that for substrate thicknesses of less than about 0.02λ, the idealized feed model provides adequate results [Ref. 23].

B. SOFTWARE MODELS

1. Method of Moments

The method of moments solves for unknown currents on the surface of the microstrip patch. If a dielectric is present, the dielectric Green's function is used to solve the electric field integral equation. This method automatically

accounts for mutual coupling and provides accurate results for antenna performance. The method of moments depends on the accurate calculation of the elements in the impedance matrix for its precision [Ref. 24] and requires a large amount of computer resource. Several methods have been developed to calculate method of moment solutions more efficiently, [Refs. 25 and 26], but comparisons with results from other models do not show significant differences [Ref. 24].

2. Modal Expansion Model

The modal expansion model was discussed in Chapter II. The limitations of this model have been shown in previous discussions to be insignificant for this application. Because of its simplicity, the modal expansion model was used to predict the performance of this antenna. The software program used for this analysis was written in FORTRAN and obtained from the Jet Propulsion Laboratory in Pasadena, CA. A source code listing for this program is contained in Appendix F.

C. MODELING SCENARIO

Using the excitation coefficients previously obtained, antenna patterns for each of the six beams were generated for scan angles of $\theta=-90°$ to $+90°$, $\phi=0$ and $\theta=-90°$ to $+90°$, $\phi=90$. The results were plotted in order to asses whether or not each beam met the design specification in terms of scan angle and beam width. A contour plot of the approximate ground

footprint of each beam was also generated in order to assess antenna ground coverage.

D. RESULTS

1. Radiation Patterns

The radiation pattern obtained for beam 1 is plotted in Figure 4.1. Beam patterns for the remaining beams are contained in Appendix G.

The model results demonstrate that both beam shape and beam orientation are attainable for beam 1. Similar results were obtained for beams 2 through 6 with one notable exception. The specification called for beams 2 and 5 to be scanned 30 degrees from center. When the beams were steered to exactly -30 degrees and 30 degrees respectively, the result resembled a broad side array beam pattern. Examination of the antenna's normal beam pattern reveals a null which prevents this antenna from being scanned to exactly 30 degrees. By adjusting the scan angle to -27 degrees for beam 2 and 27 degrees for beam 5, acceptable beam patterns were obtained.
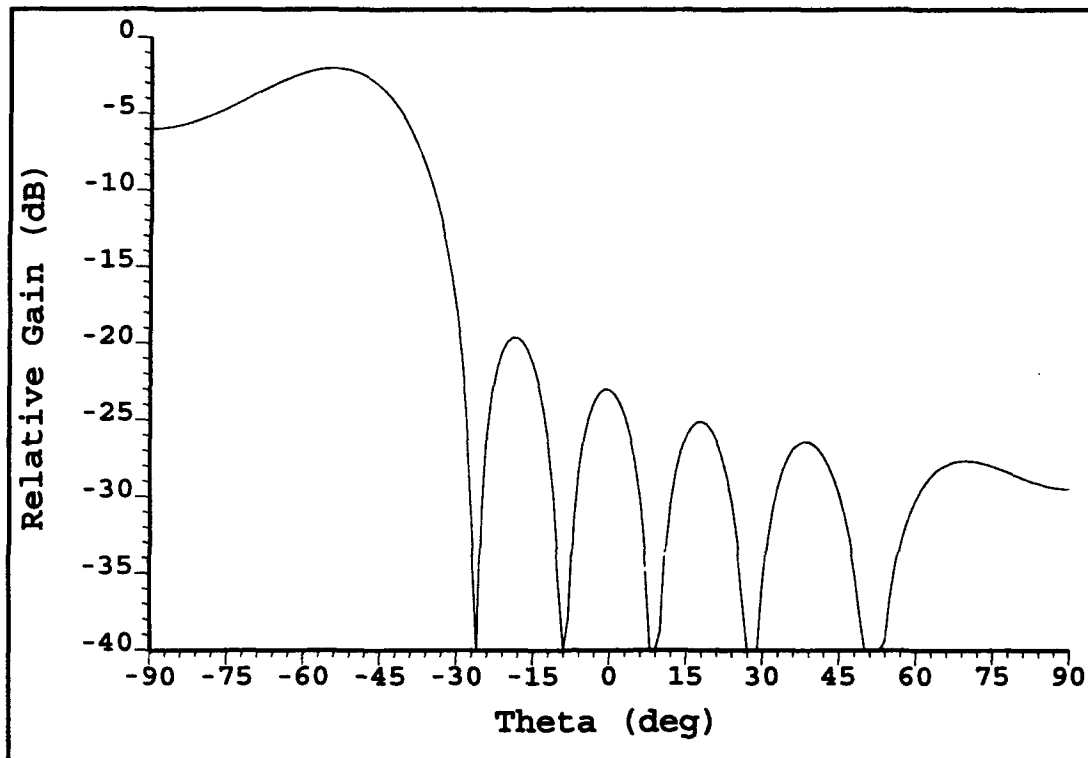
Figure 4.1. Beam 1 Radiation Pattern (φ=90°)

2. Pattern Separation

Recall that the beams are required to operate in transmit/receive pairs such that the satellite uplink and downlink can be operated simultaneously at the same frequency. This requires adequate pattern separation to avoid mutual interference at the earth's surface. Figure 4.2 demonstrates that this design achieves adequate pattern separation for beams 1 and 4. Similar results were obtained for beam pair 2 and 5 and pair 3 and 6 and are presented in Appendix G.
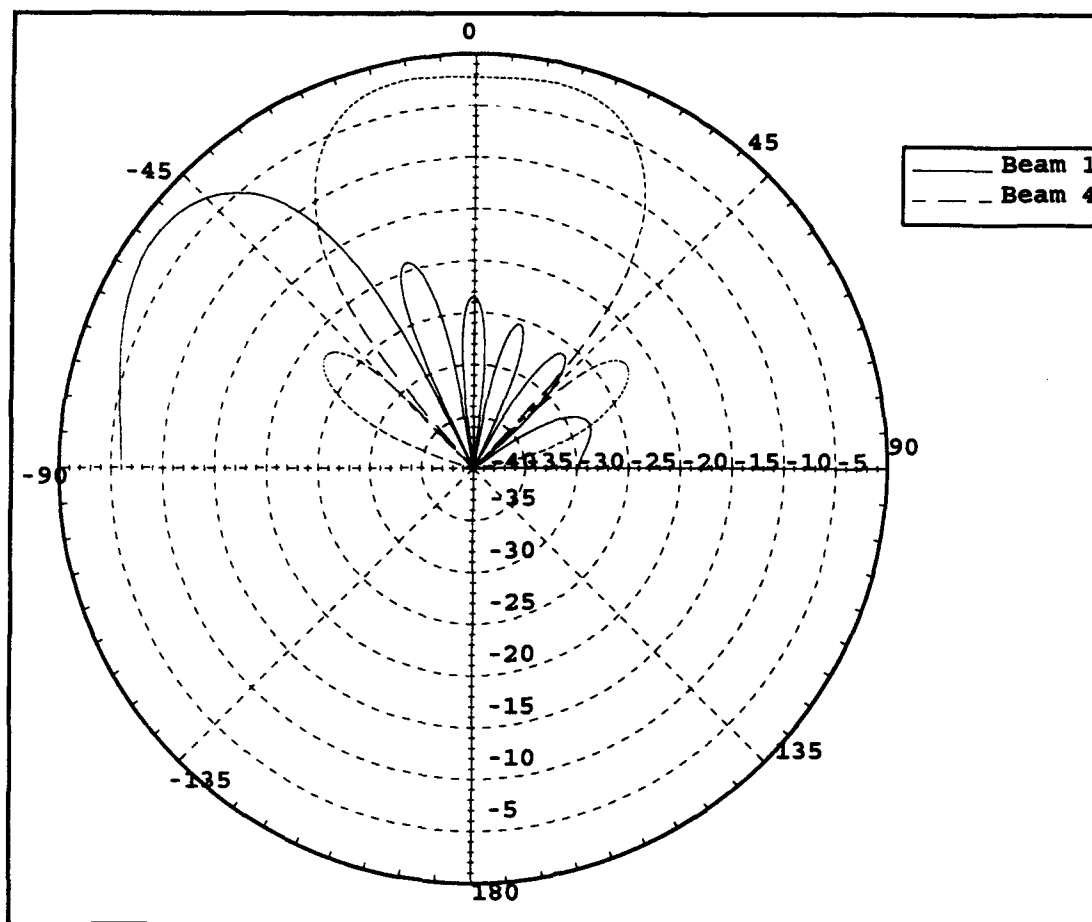
Figure 4.2. Simultaneous Beam Patterns

3. Antenna Footprint

In order to clearly demonstrate antenna coverage, the relative gain for each beam was computed over a 5 degree by 5 degree grid centered about the satellite's nadir. The results for beam 2 are presented in Figure 4.3. The beam pattern is shown in terms of scan angle from nadir in the in-track and cross-track directions. Similar results were obtained for the remaining beams and are contained in Appendix G.

Relative dB Contours
(Beam scanned 27 degrees from nadir)
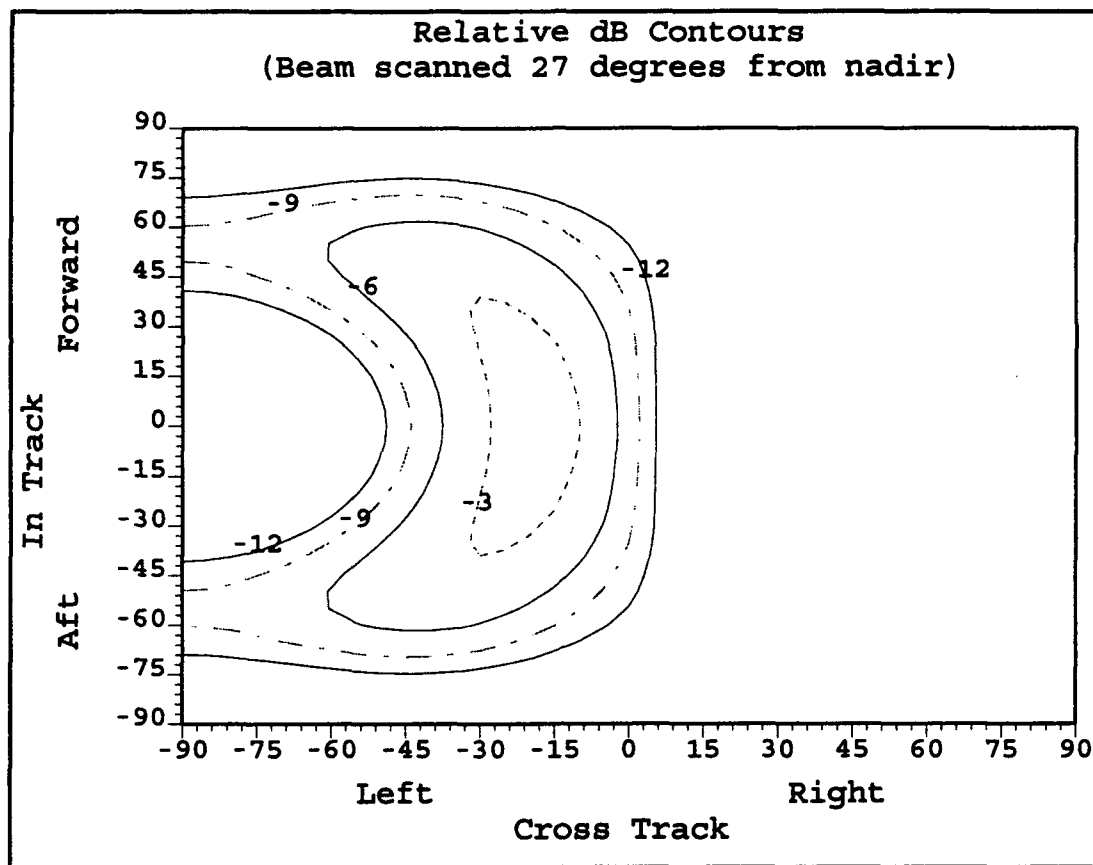
Figure 4.3. Beam 2 Relative dB Gain Footprint

V. ALTERNATIVE DESIGN

A. ANTENNA CONFIGURATION

An alternative design to that presented in the previous chapters is one which takes advantage of the fact that the L-band communications signal uses time division multiplexing (TDM). The use of TDM, as implemented in the payload for this spacecraft, means that each of the six antenna beams has a 60 ms duty cycle. Since adjacent pairs of antennas are not operating at the same time, the antenna could be constructed such that there are two beams per antenna panel thus reducing the number of panels required.

An integrated multiple beam microstrip array similar to that described in [Ref. 27] could be constructed. Two feed lines would be constructed on a lower substrate which would be electromagnetically coupled to the patch array on the substrate above. Each feed line would be energized at the appropriate time corresponding to the on-time for the particular beam. This configuration would simplify antenna construction by eliminating the need for through-hole plating and connecting pins between the feed network and the patch elements [Ref. 28]. The deployment mechanism for this configuration would also be much simpler as only two hinged panels would have to unfold as opposed to four. There would also be a reduction in weight while performance would actually

be enhanced due to reduced losses in the smaller feed network required.

Combining two antenna panels into one and using that single panel for two beams would almost double the number of patch elements available to each beam. In addition to increasing gain, this would allow better resolution in both beam shape and orientation. Increasing the number of array elements would also eliminate unwanted nulls which adversely affect scan angle.

B. ANTENNA ORIENTATION

The antenna in this study is oriented such that individual panels are perpendicular to the spacecraft's velocity vector. This orientation was chosen for structural and thermal control reasons during the early stages of the preliminary design and is not optimum. If the design described above were adopted, the antenna panels could be oriented parallel to the velocity vector allowing cross track beam steering to be accomplished by tilting two outside panels towards the center. All available patch elements could then be dedicated to shaping the beam which would result in reduced beam overlap.

VI. SUMMARY

A. ANALYSIS AND DESIGN

Two different substrate materials were considered for the design of a multiple beam, phased array, microstrip antenna. Design curves were presented to illustrate tradeoffs between weight and performance in the substrate material. This information was used to choose an appropriate substrate material which would provide adequate performance at a minimum cost in mass.

Closed form formulae were used to arrive at a preliminary width and length for microstrip patch elements. A computer model was then used to optimize the width and length dimensions. Array theory was applied to derive patch excitation coefficients.

B. PERFORMANCE EVALUATION

Patch excitation coefficients were used as input to a computer model, which employs modal expansion theory, and antenna radiation patterns were generated.

While the Method of Moments would have yielded more accurate results, it would have been at the expense of increased computer time. The Modal Expansion method used provided adequate results with a reasonable amount of effort.

40

The results demonstrate that the proposed design would not meet all the design goals. While the desired beam shapes were obtained, the ground footprint of the outside beams (beam 1 and 6) show that most of the energy would be concentrated outside the satellite's field of view.

C. CONCLUSIONS

Analysis showed that this antenna could not be constructed within the allocated mass budget. In fact, the mass of the substrate material alone would be over two times the allocated mass budget.

The use of rectangular microstrip patches is not an efficient use of the available array area. An octagonally shaped patch would allow more elements to be placed on a panel. This would allow tighter control over beam shape and orientation.

The alternative design discussed in Chapter IV would address the short-comings in the original design and allow the ground footprint to be entirely within the satellite's field of view. However, operating two beams per antenna panel could require active phase shifters, increasing cost as well as reliability risk.

The use of fiber optic cables instead of coaxial transmission line and etched copper feed networks would reduce both weight and power loss.

Since the methods for determining patch dimensions discussed in the literature all give slightly different results, this antenna would have to be tested and trimmed after construction in order to ensure the operating parameters were met.

D. FUTURE THESIS OPPORTUNITIES

A scale model could be built and tested by increasing the operating frequency to yield a smaller wavelength. The coupled feed model discussed in the alternative design could also be built and tested. Various orientations, beam patterns, and scan angle could be explored yielding useful data for future phased array design projects.

APPENDIX A

LINK BUDGET SUMMARY

TABLE A-1. LINK BUDGET [REF. 1]

	User to Satellite			Satellite to User	
Frequency	1625.0	MHz	Frequency	1625.0	MHz
RF Power	6	Watts	RF Power	19	Watts
	7.8	dBw		12.8	dBw
Power Loss	-1.0	dB	Power Loss	-2.2	db
Antenna Gain	3.0	DBi	S/C Ant. Gain (isoflux)	4.0-6.0	dBi
EIRP	9.8	dBw	EIRP	14.6	dBw
Satellite Altitude- 750 NM	1389.0	km	Satellite Altitude	1389.0	km
Elevation Angle	90.0	degrees	Elevation Angle	90.0	degrees
Range	1389.0	km	Range	1389.0	km
Free Space Loss	-159.5	dB	Free Space Loss	-159.5	dB
RX Signal Strength	-149.8		RX Signal Strength	-155.9	
Polarization Loss	-0.5	dB	Polarization Loss	-0.5	dB
Tracking Loss	0.0	dB	Tracking Loss	0.0	dB
S/C Ant. Gain (isoflux)	4.0-6.0	dBi	Antenna Gain	3.0	dBi
RX Line Losses	-1.0	dB	RX Line Loss	-0.5	dB
L-Band Amplifier Eff.	35	%	L-Band Amplifier Eff.	35	%
E_b/N_0 Required	3.5	dB	E_b/N_0 Required	3.5	dB
Total BW	16.5	MHz	Total BW	16.5	MHz

APPENDIX B

I. MASS ESTIMATES

A. Kevlar Subtrate

Density = 0.05 lb/in^3 Density = 1.4 gm/cm^3

The total substrate volume is given by:

l = 1.4 m   w = 0.667 m   h = 0.003 m

Volume = l x w x h x 2 x 6

Volume = 3.4 x 10^4 cm^3

The total substrate mass is given by:

Mass$_{Kevlar}$ = Volume x Density

Mass$_{Kevlar}$ = 46.5 Kg   Mass$_{Kevlar}$ = 102.6 lb

B. Duroid Substrate

Specific_gravity = 2.2   Density = 2.2 gm/cm^3

Total substrate mass:

Mass$_{Duroid}$ = Volume x Density

Mass$_{Duroid}$ = 74 Kg   Mass$_{Duroid}$ = 163 lb

C.   Copper

1.   Microstrip Patches

$$Density_{Cu} = 8.96 \ gm/cm^3$$

Total number of elements = 9 x 4 x 6 = 216

Element width = 5.9 cm   Element length = 4.6 cm

$Thickness_{Cu} = 0.0127$ cm

Total volume of array elements = length x width x $thickness_{Cu}$ x tot num elements

Total volume = 74.5 cm^3

Total $Mass_{elements}$ = Density x volume

Total $Mass_{elements}$ = 0.7 Kg

2.   Microstrip Feed Lines

$$length_{feed} = 1.3 \ m \qquad width_{feed} = 0.006 \ m$$

$Volume_{feed}$ = $length_{feed}$ x $width_{feed}$ x $thickness_{Cu}$

$Mass_{feed}$ = $Density_{Cu}$ x $Volume_{feed}$

$Mass_{feed}$ = 8.9×10^{-4} Kg

3.   Total Copper Mass

The total copper mass is given by:

$Mass_{Cu}$ = $Mass_{elements}$ + $Mass_{feed}$

$Mass_{Cu}$ = 0.701 Kg

D.   Aluminum Ground Planes

Since a shielded triplate feed is used, two aluminum ground planes are needed.

$Density_{Al}$ = 2.7 gm/cm^3 $\qquad$ $thickness_{Al}$ = 1.0×10^{-4}

$Volume_{Al}$ = l x w x $thickness_{Al}$ x 4

45

$$\text{Mass}_{Al} = \text{Volume}_{Al} \times \text{Density}_{Al} \times 2$$

$$\text{Mass}_{Al} = 1.35 \times 10^{-3} \text{ Kg}$$

II. SUMMARY

The Duroid substrate is approximately 1.5 times heavier than the Kevlar for a given volume. Therefore, the Kevlar material should be used for the substrate. The total mass for the antenna is estimated as follows:

$$\text{Mass} = \text{Mass}_{Kevlar} + \text{Mass}_{Cu} + \text{Mass}_{Al}$$

A mass margin of 0.01 is chosen and the total antenna mass becomes

$$\text{Mass}_{antenna} = \text{Mass} \times (1 + \text{Mass}_{margin})$$

$$\text{Mass}_{antenna} = 52 \text{ Kg} \qquad \text{Mass}_{antenna} = 114.5 \text{ lb}$$

APPENDIX C

I. PATCH DESIGN

Using the transmission line model, the patch parameters are calculated as follows:

Given: f = 1618.25 MHz ε_r = 3.9   h=0.3 cm

l = 3(10)^8/f   k = 2π/λ

λ = 18.5 cm   k = 33.9

$$W = \frac{c}{2f_r}\left[\frac{\varepsilon_r+1}{2}\right]^{-\frac{1}{2}} \quad (cm)$$

W = 5.9 cm

The effective dielectric constant is given by:

$$\varepsilon_e = \frac{\varepsilon_r+1}{2} + \frac{\varepsilon_r-1}{2}\left(1+\frac{12h}{W}\right)^{-\frac{1}{2}}$$

ε_e = 3.6

The patch length is then calculated as follows:

$$\Delta l = 0.412h \frac{(\varepsilon_e+0.3)(\frac{W}{h}+0.264)}{(\varepsilon_e-0.258)(\frac{W}{h}+0.8)}$$

Δl = 0.1 cm

$$L = \frac{c}{2f_r\sqrt{\varepsilon_e}} - 2\Delta l \quad (cm)$$

L = 4.6 cm

II.   GAIN

In order to calculate gain, the directivity must be calculated according to the following:

$$D_0 = \frac{4W^2\pi^2}{\int \sin(\frac{kW\cos(\theta)}{2})^2 \tan(\theta)^2 \sin(\theta)\, d\theta\ \lambda^2}$$

Losses, expressed as resistance, must also be found according to the following relations:

Quality factor:

$$Q = \frac{3(10)^8 \sqrt{\varepsilon_e}}{4\ f\ h}$$

Radiation resistance: $R_r = 120\lambda/W$

Copper loss:

$$R_c = 2.7(10)^{-4} \sqrt{(\frac{f}{10^3})(\frac{L}{W})}\ Q^2$$

Dielectric loss:

$$R_d = \frac{81(10)^{-3}}{\varepsilon_e} \frac{h\ \lambda}{L\ W}\ Q^2$$

The total resistance is then $R_T = R_r + R_c + R_d$ $R_T = 379.8$
With a of VSWR = 2, Bandwidth (BW) and efficiency (η) are found as follows:

$$BW = \frac{(VSWR - 1)}{(Q\sqrt{VSWR})} \times 100 \qquad\qquad \eta = \frac{R_r}{R_T}$$

Directivity and Gain are computed as:

$D = 10 \times \log(D_0)$ $D = 5.06\ dB$

$G = 10 \times \log(\eta \times D_0)$ $G = 5.0\ dB$

APPENDIX D

EXCITATION COEFFICIENTS

TABLE D-1. BEAM 1 EXCITATION COEFFICIENTS

Element Number	1	2	3	4
1	0.013 ∠52.36°	0.046 ∠-127.6°	0.046 ∠-127.6°	0.013 ∠52.36°
2	0.019 ∠-57.73°	0.066 ∠129.3°	0.066 ∠129.3°	0.019 ∠-57.73°
3	0.024 ∠-153.8°	0.083 ∠28.18°	0.083 ∠28.18°	0.024 ∠-153.8°
4	0.027 ∠103.1°	0.094 ∠-76.9°	0.094 ∠-76.9°	0.027 ∠103.1°
5	0.028 ∠0.0°	0.098 ∠180.0°	0.098 ∠-180.0°	0.028 ∠0.0°
6	0.027 ∠-103.1°	0.094 ∠76.9°	0.094 ∠76.9°	0.027 ∠-103.1°
7	0.024 ∠153.8°	0.083 ∠-28.18°	0.083 ∠-28.18°	0.024 ∠153.8°
8	0.019 ∠57.73°	0.066 ∠-129.3°	0.066 ∠-129.3°	0.019 ∠57.73°
9	0.013 ∠-52.36°	0.046 ∠127.6°	0.046 ∠127.6°	0.013 ∠-52.36°

TABLE D-2. BEAM 2 EXCITATION COEFFICIENTS

Element Number	1	2	3	4
1	0.003 ∠169.3°	0.010 ∠-10.68°	0.010 ∠-10.68°	0.003 ∠169.3°
2	0.011 ∠-55.0°	0.039 ∠127.0°	0.039 ∠127.0°	0.011 ∠-55.0°
3	0.029 ∠-95.3°	0.099 ∠84.6°	0.099 ∠84.6°	0.029 ∠-95.3°
4	0.043 ∠-137.7°	0.148 ∠42.3°	0.148 ∠42.3°	0.043 ∠-137.7°
5	0.048 ∠-180.0°	0.167 ∠0.0°	0.167 ∠0.0°	0.048 ∠180.0°
6	0.043 ∠137.7°	0.148 ∠-42.3°	0.148 ∠-42.3°	0.043 ∠137.7°
7	0.029 ∠95.3°	0.081 ∠-84.6°	0.099 ∠-84.6°	0.029 ∠95.3°
8	0.011 ∠53.0°	0.039 ∠-127.0°	0.039 ∠-127.0°	0.011 ∠53.0°
9	0.003 ∠-169.3°	0.010 ∠10.68°	0.010 ∠10.68°	0.003 ∠-169.3°

TABLE D-3. BEAM 3 EXCITATION COEFFICIENTS

Element Number	1	2	3	4
1	0.013 ∡7.7°	0.046 ∡-172.3°	0.046 ∡-172.3°	0.013 ∡7.7°
2	0.002 ∡5.8°	0.007 ∡-174.2°	0.007 ∡-174.2°	0.002 ∡5.8°
3	0.024 ∡-176.1°	0.083 ∡3.8°	0.083 ∡3.8°	0.024 ∡-176.1°
4	0.051 ∡-178.1°	0.176 ∡1.9°	0.176 ∡1.9°	0.051 ∡-178.1°
5	0.062 ∡-180.0°	0.215 ∡0.0°	0.215 ∡0.0°	0.062 ∡180.0°
6	0.051 ∡178.1°	0.176 ∡-1.9°	0.176 ∡-1.9°	0.051 ∡178.1°
7	0.024 ∡176.1°	0.083 ∡-3.8°	0.083 ∡-3.8°	0.024 ∡176.1°
8	0.002 ∡-5.8°	0.007 ∡174.2°	0.007 ∡174.2°	0.002 ∡-5.8°
9	0.013 ∡-7.7°	0.046 ∡172.3°	0.046 ∡172.3°	0.013 ∡-7.7°

TABLE D-4. BEAM 4 EXCITATION COEFFICIENTS

Element Number	1	2	3	4
1	0.013 $\angle-7.7°$	0.046 $\angle172.3°$	0.046 $\angle172.3°$	0.013 $\angle-7.7°$
2	0.002 $\angle-5.8°$	0.007 $\angle174.2°$	0.007 $\angle174.2°$	0.002 $\angle-5.8°$
3	0.024 $\angle176.1°$	0.083 $\angle-3.8°$	0.083 $\angle-3.8°$	0.024 $\angle176.1°$
4	0.051 $\angle178.1°$	0.176 $\angle-1.9°$	0.176 $\angle-1.9°$	0.051 $\angle178.1°$
5	0.062 $\angle-180.0°$	0.215 $\angle0.0°$	0.215 $\angle0.0°$	0.062 $\angle180.0°$
6	0.051 $\angle-178.1°$	0.176 $\angle1.9°$	0.176 $\angle1.9°$	0.051 $\angle-178.1°$
7	0.024 $\angle-176.1°$	0.083 $\angle3.8°$	0.083 $\angle3.8°$	0.024 $\angle-176.1°$
8	0.002 $\angle5.8°$	0.007 $\angle-174.2°$	0.007 $\angle-174.2°$	0.002 $\angle5.8°$
9	0.013 $\angle7.7°$	0.046 $\angle-172.3°$	0.046 $\angle-172.3°$	0.013 $\angle7.7°$

TABLE D-5. BEAM 5 EXCITATION COEFFICIENTS

Element Number	1	2	3	4
1	0.003 ∠-169.3°	0.010 ∠10.68°	0.010 ∠10.68°	0.003 ∠-169.3°
2	0.011 ∠55.0°	0.039 ∠-127.0°	0.039 ∠-127.0°	0.011 ∠55.0°
3	0.029 ∠95.3°	0.099 ∠-84.6°	0.099 ∠-84.6°	0.029 ∠95.3°
4	0.043 ∠137.7°	0.148 ∠-42.3°	0.148 ∠-42.3°	0.043 ∠137.7°
5	0.048 ∠-180.0°	0.167 ∠0.0°	0.167 ∠0.0°	0.048 ∠180.0°
6	0.043 ∠-137.7°	0.148 ∠42.3°	0.148 ∠42.3°	0.043 ∠-137.7°
7	0.029 ∠-95.3°	0.081 ∠84.6°	0.099 ∠84.6°	0.029 ∠-95.3°
8	0.011 ∠-53.0°	0.039 ∠127.0°	0.039 ∠127.0°	0.011 ∠-53.0°
9	0.003 ∠169.3°	0.010 ∠-10.68°	0.010 ∠-10.68°	0.003 ∠169.3°

TABLE D-6. BEAM 6 EXCITATION COEFFICIENTS

Element Number	1	2	3	4
1	0.013 ∠-52.36°	0.046 ∠127.6°	0.046 ∠127.6°	0.013 ∠-52.36°
2	0.019 ∠57.73°	0.066 ∠-129.3°	0.066 ∠-129.3°	0.019 ∠57.73°
3	0.024 ∠153.8°	0.083 ∠-28.18°	0.083 ∠-28.18°	0.024 ∠153.8°
4	0.027 ∠-103.1°	0.094 ∠76.9°	0.094 ∠76.9°	0.027 ∠-103.1°
5	0.028 ∠0.0°	0.098 ∠180.0°	0.098 ∠-180.0°	0.028 ∠0.0°
6	0.027 ∠103.1°	0.094 ∠-76.9°	0.094 ∠-76.9°	0.027 ∠103.1°
7	0.024 ∠-153.8°	0.083 ∠28.18°	0.083 ∠28.18°	0.024 ∠-153.8°
8	0.019 ∠-57.73°	0.066 ∠129.3°	0.066 ∠129.3°	0.019 ∠-57.73°
9	0.013 ∠52.36°	0.046 ∠-127.6°	0.046 ∠-127.6°	0.013 ∠52.36°

APPENDIX E

ARRAY FACTOR PLOTS
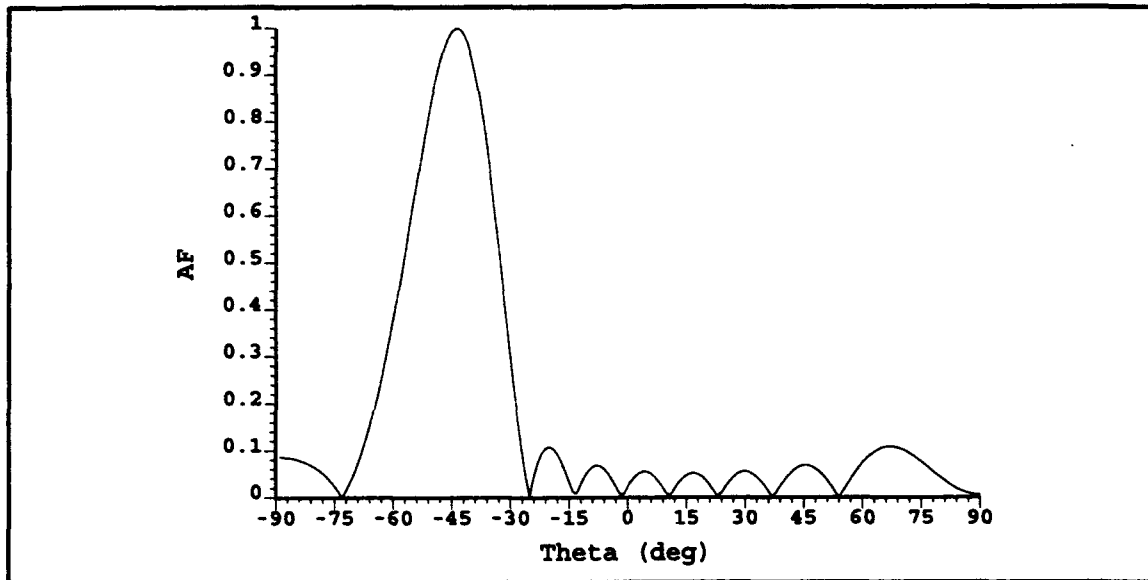
Figure E-1.   Beam 1 Array Factor (ϕ=90°)
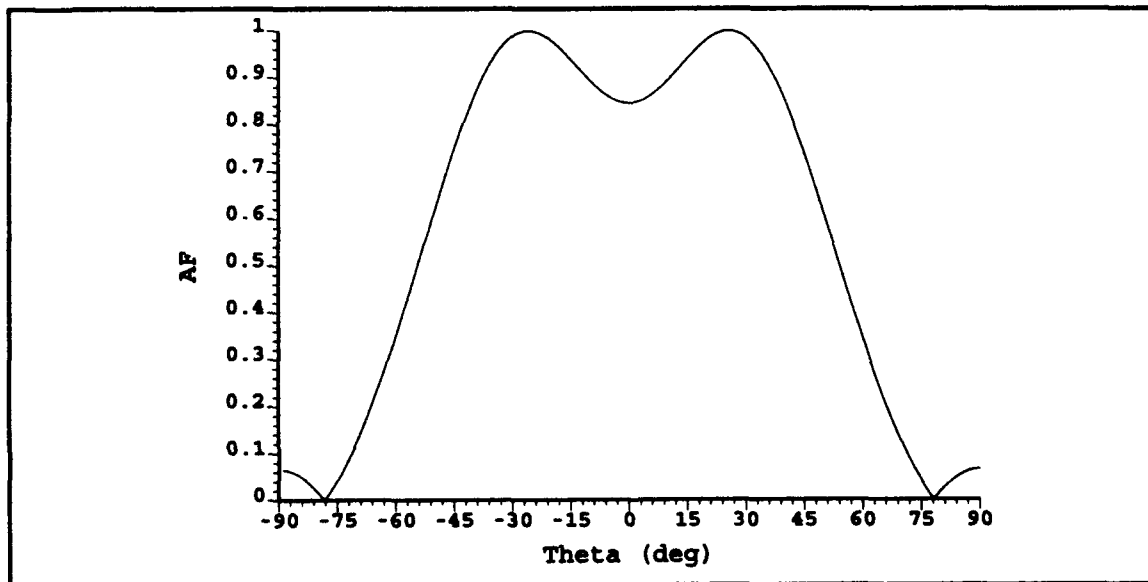
Figure E-2.   Beam 1 Array Factor (ϕ=0°)
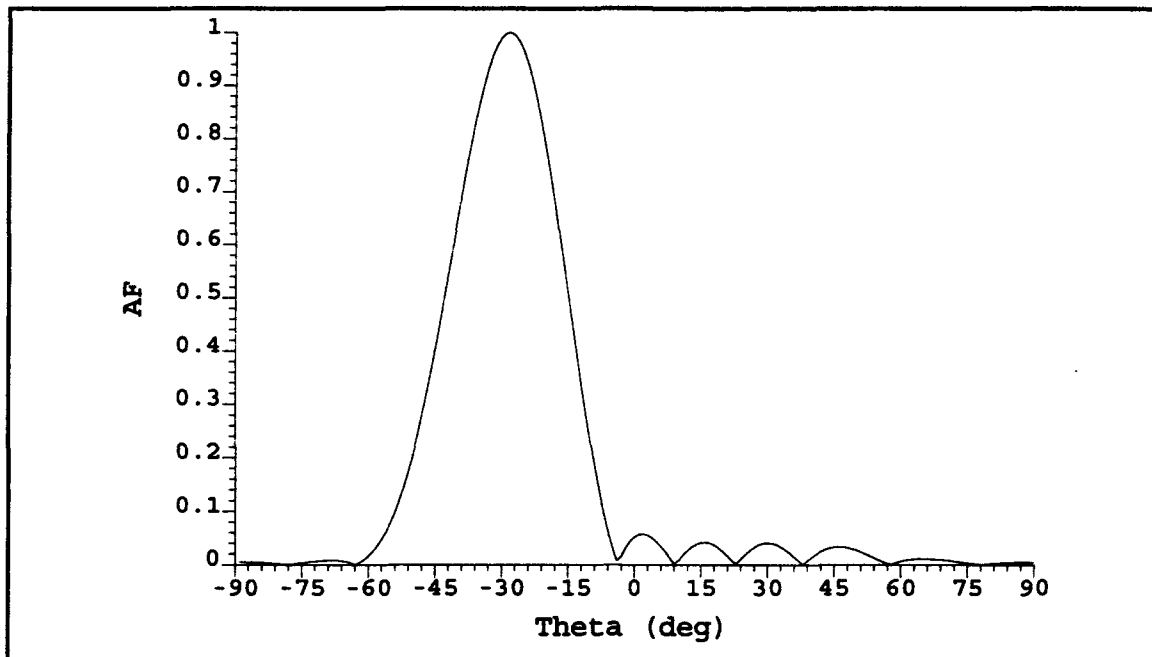
Figure E-3. Beam 2 Array Factor (φ=90°)
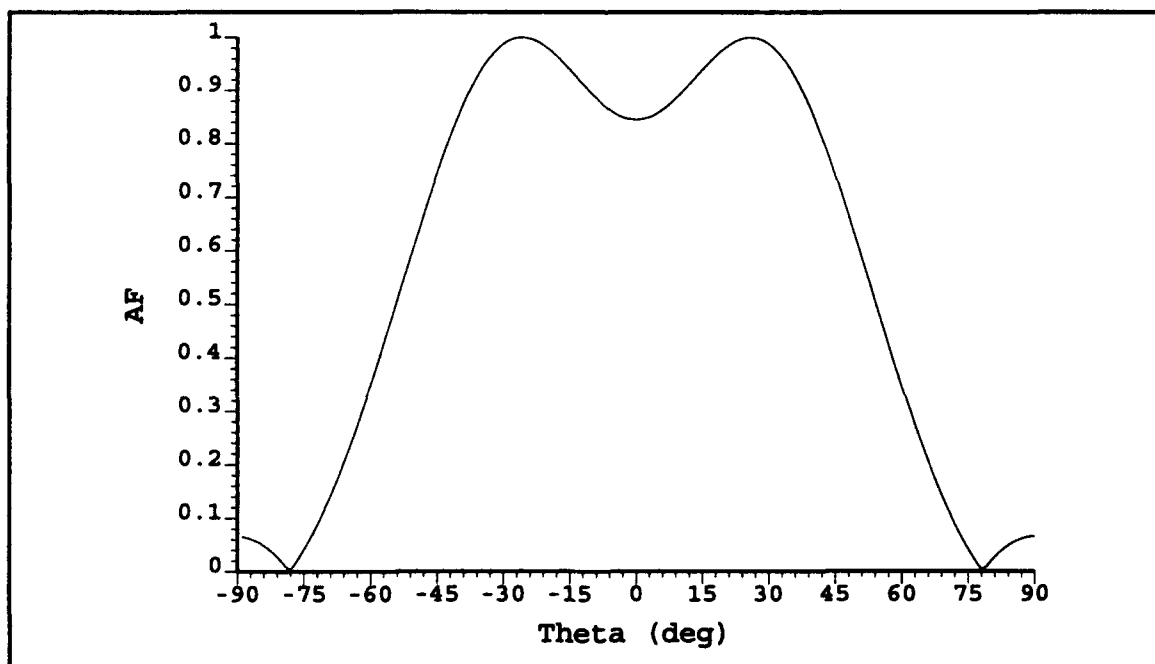
Figure E-4. Beam 2 Array Factor (φ=0°)

56
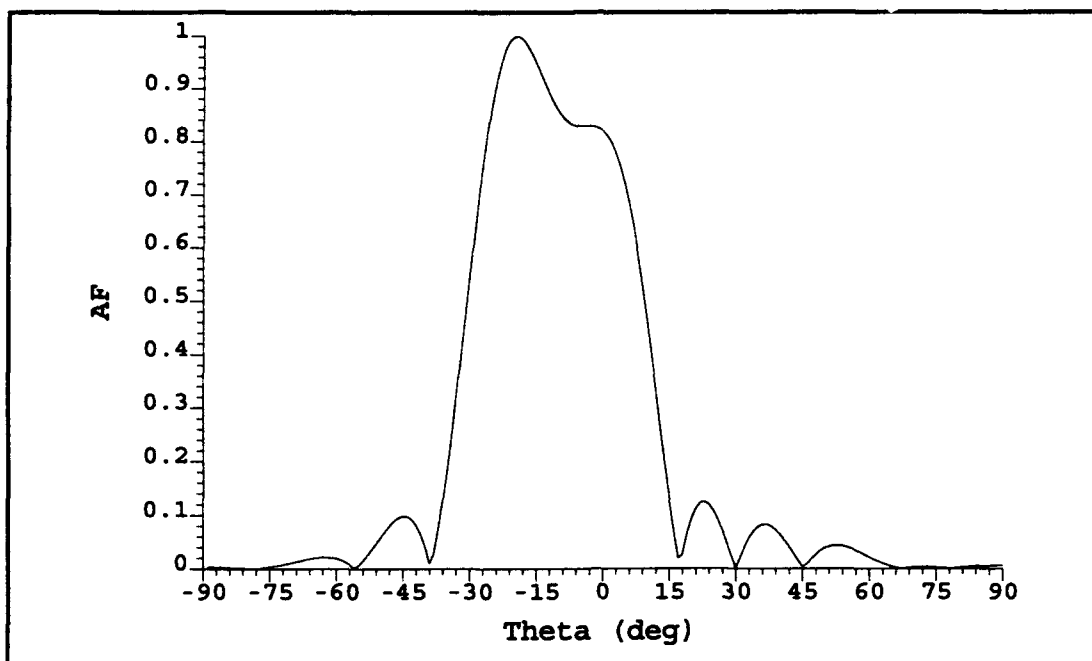
Figure E-5. Beam 3 Array Factor (φ=90)
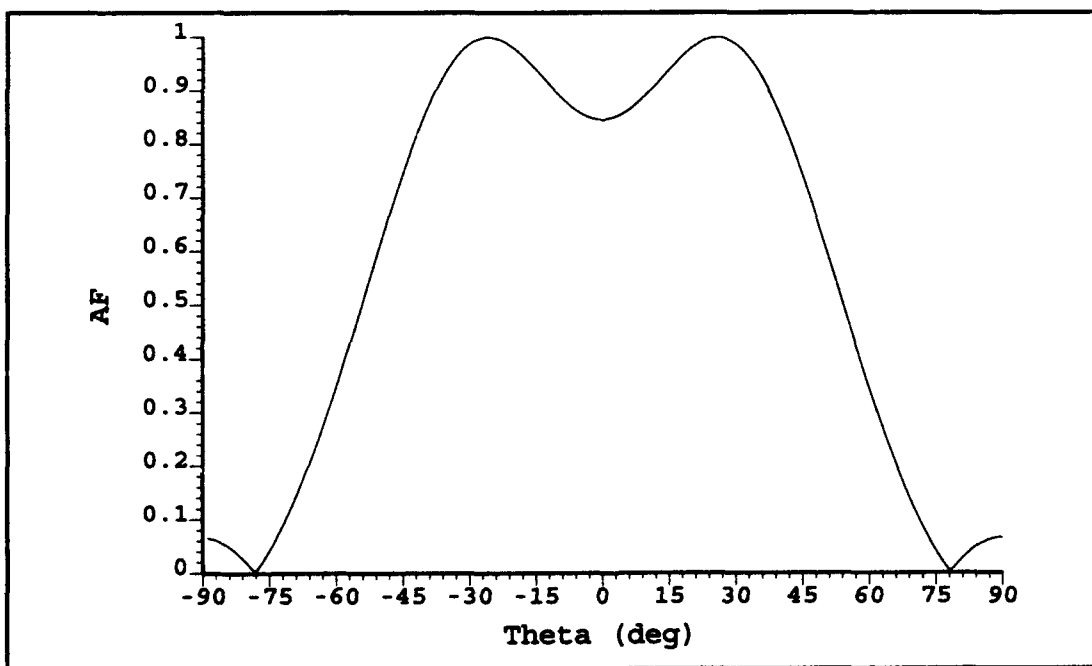
Figure E-6. Beam 3 Array Factor (φ=0°)
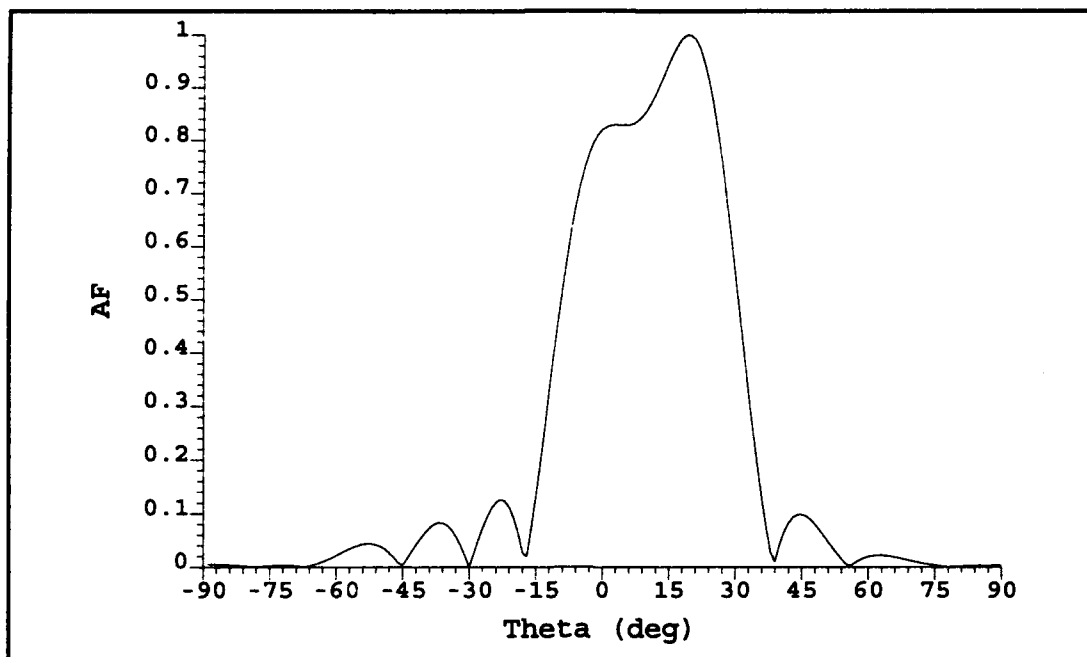
Figure E-7. Beam 4 Array Factor ($\phi=90°$)
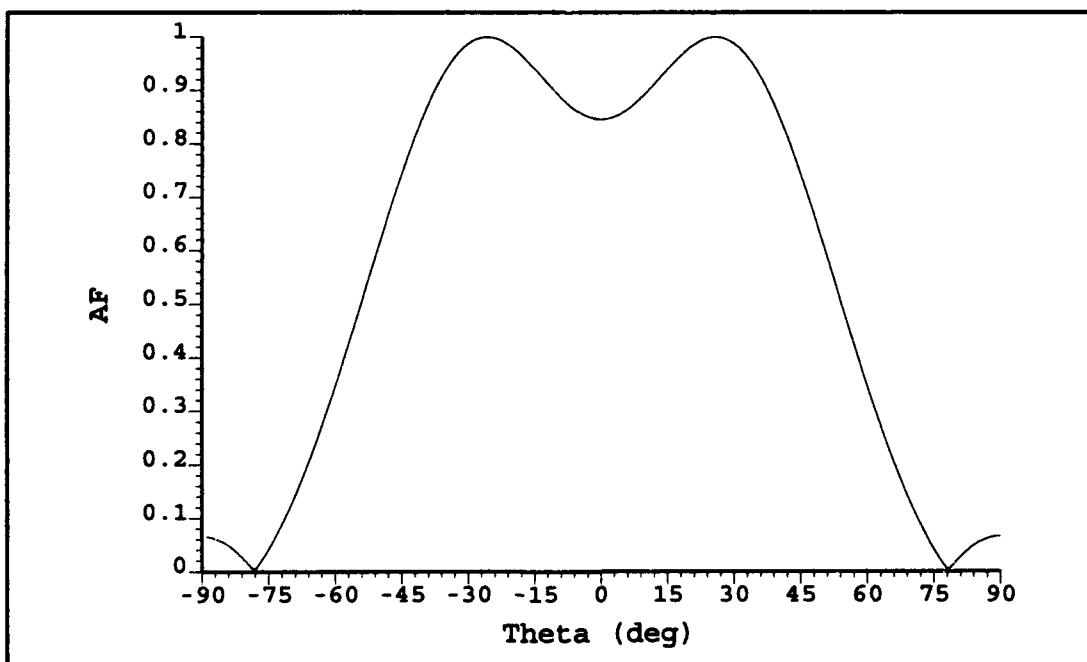
Figure E-8. Beam 4 Array Factor ($\phi=0°$)
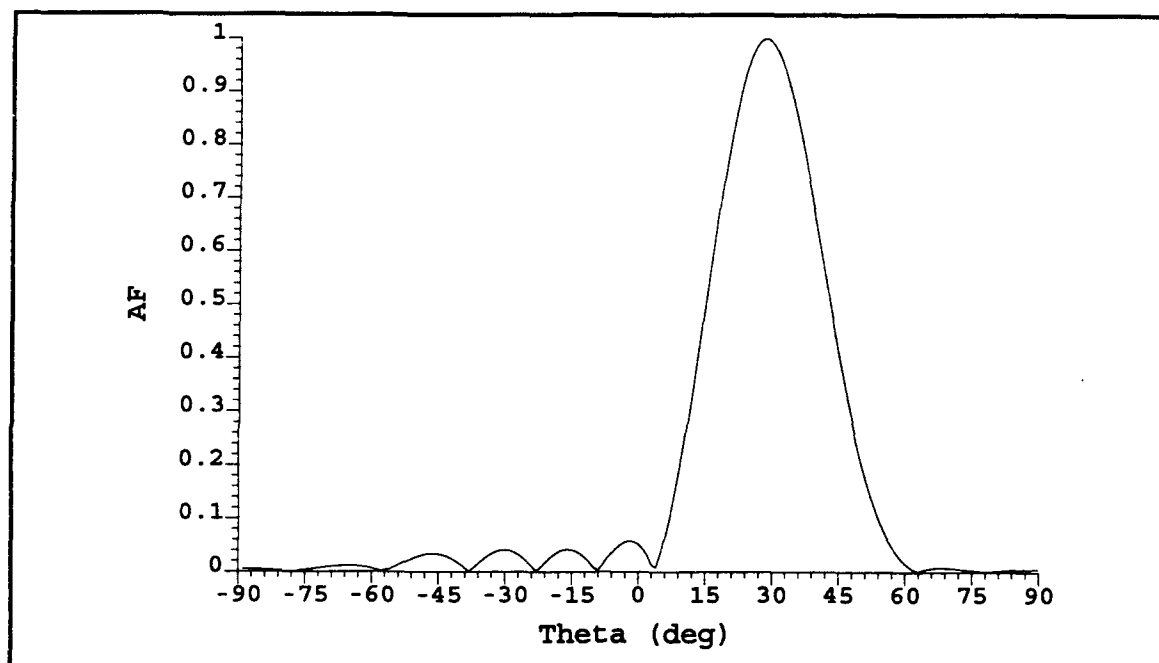
Figure E-9.   Beam 5 Array Factor ($\phi=90°$)
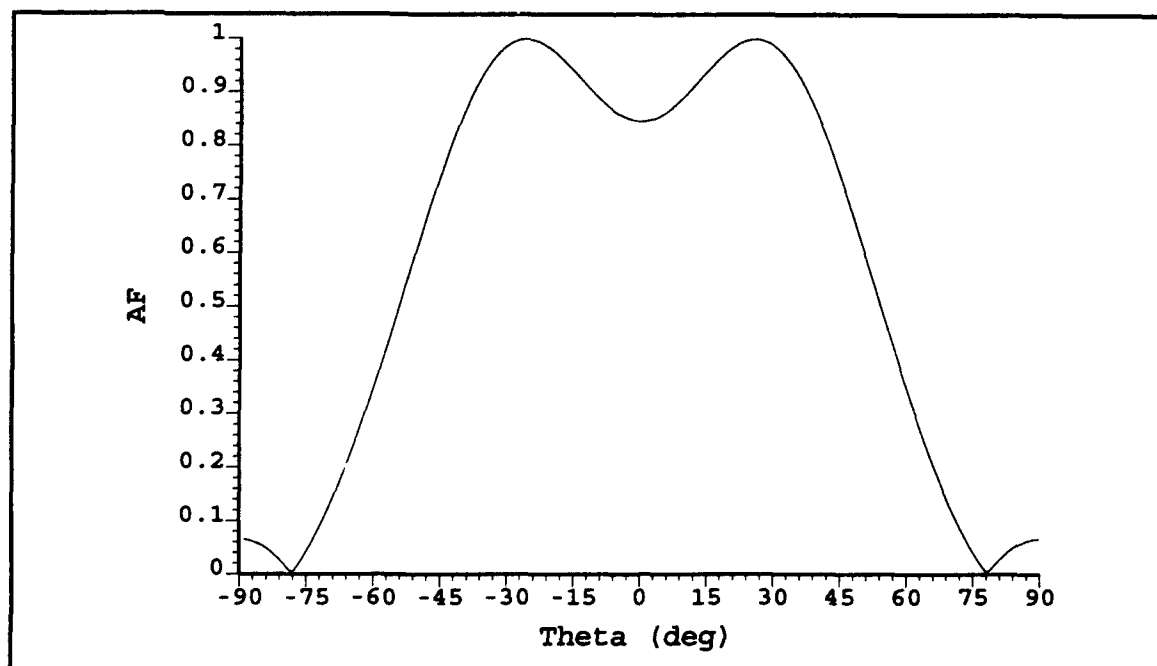
Figure E-10.   Beam 5 Array Factor ($\phi=0°$)
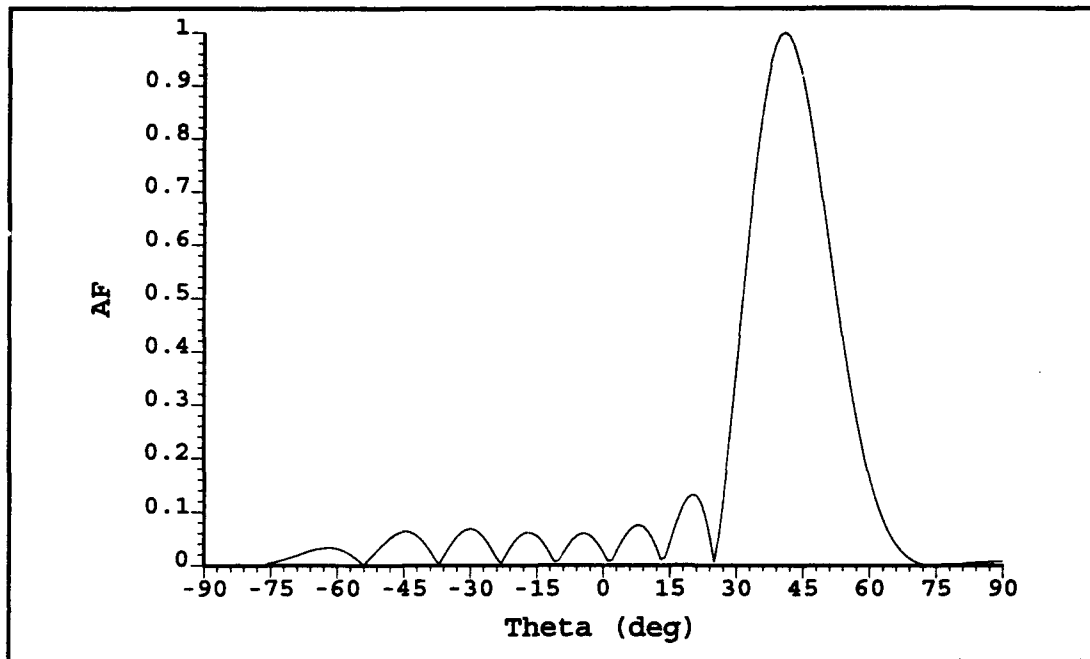
Figure E-11.   Beam 6 Array Factor (ϕ=90°)
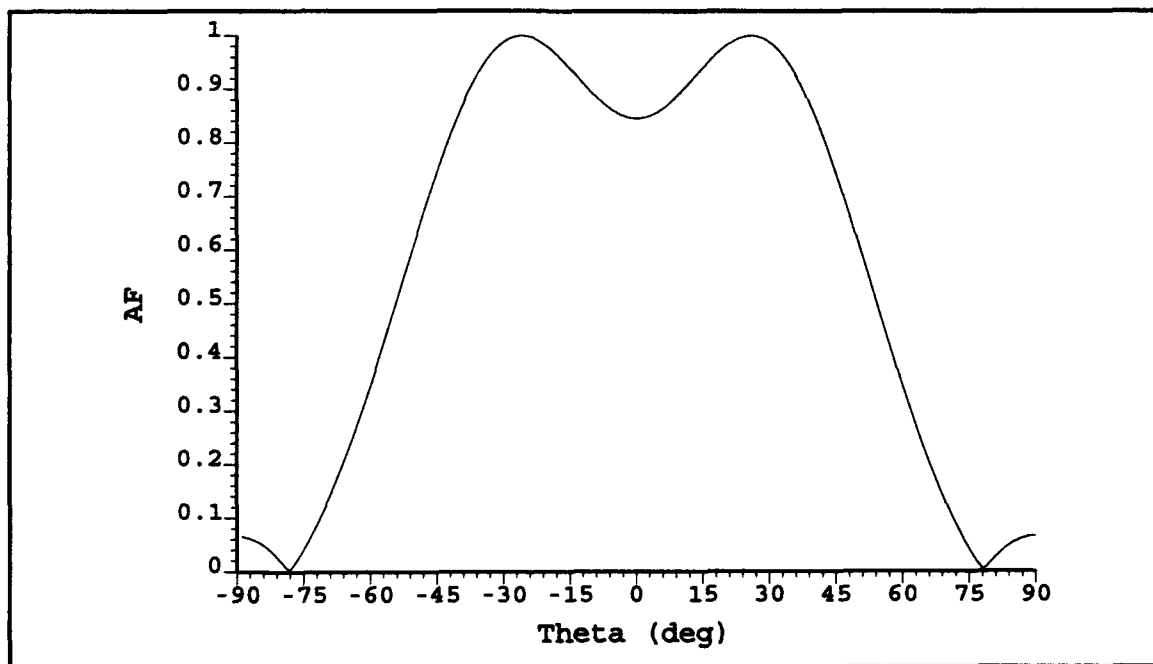
Figure E-12.   Beam 6 Array Factor (ϕ=0°)

60

APPENDIX F

I. DESIGN.FOR

```
C...MICROSTRIP ANTENNA DESIGN CHARACTERISTICS CALCULATED BY
    MODAL
C...THEORY, ALL INPUT LENGTH ARE IN CENTIMETER, BY DR. HUANG
        COMPLEX CJ,YWY,AY,DEL(5),C1,C2,D4,SKY,FC,WC
        REAL A,B,EPS
        CJ=(0.,1.)
        PI=3.14159265
        TPI=2.*PI
        DPR=180./PI

        TOL=.0001

        WRITE(6,11)
 11     FORMAT(' CENTER FREQ=?')
        READ(5,99)FREQ
        WRITE(6,1)
 1      FORMAT(' WIDTH OF PATCH=?')
        READ(5,99)A
 99     FORMAT(F5.8)
        WRITE(6,2)
 2      FORMAT(' RESONANT LENGTH OF PATCH=?')
        READ(5,99)B
        WRITE(6,3)
 3      FORMAT(' DIELECTRIC CONSTANT=?')
        READ(5,99)EPS
        WRITE(6,4)
 4      FORMAT(' DIELECTRIC THICKNESS=?')
        READ(5,99)T
        WRITE(6,5)
 5      FORMAT(' PROBE LOCATION=?')
        READ(5,99)YO
        WRITE(6,6)
 6      FORMAT(' LOSS TANGENT=?')
        READ(5,99)TLOS
 40     FF=1./SQRT(1.+10.*T/A)
        EPE=(EPS+1.)/2.+(EPS-1.)/2.*FF
        FF=(A/T+0.262)/(A/T+0.813)*(EPE+0.3)/(EPE-0.258)*0.412
        WAMDA=2.1*B*SQRT(EPS)
        GW=0.00836*A/WAMDA
        BW=0.01668*FF*A*EPE/WAMDA
        FY=0.7747+0.5977*(A/B-1.)-0.1638*(A/B-1.)**2.
        YWY=CMPLX(GW,BW)
```

```fortran
      AY=CJ*TPI*376.7/WAMDA*T/A*YWY*FY*B
      DEL(1)=(0.,0.)
      DO 20 I=1,4
      C1=2.*AY*(CMPLX(PI,0.)-DEL(I))
      C2=AY*AY+2.*DEL(I)*PI-DEL(I)*DEL(I)-CMPLX(PI*PI,0.)
      DEL(I+1)=C1/C2-(DEL(I))**3./3.
20    CONTINUE
      D4=DEL(5)
      SKY=(CMPLX(PI,0.)-D4)/B
      FC=CMPLX(1.,0.)-CJ*TLOS
      WC=3.E10/SQRT(EPS*FC)*SKY
      FR=REAL(WC)/TPI
      QR=REAL(WC)/2./AIMAG(WC)
      FF=COS(PI*YO/B)
      CC=EPE*8.854*1.E-14*A*B/2./T/FF/FF
      RAD=QR/REAL(WC)/CC
      RCU=0.00027*SQRT(FR/1.E+9)*B/A*QR*QR
      RDI=30.*TLOS*T*WAMDA/EPS/A/B*QR*QR
      RIN=RAD+RCU+RDI
      Q=RIN*REAL(WC)*CC
      DFR=FR/Q
      EFF=RAD/RIN
      FR=FR/1.E+9

      DFREQ=FREQ-FR
      IF((ABS(DFREQ)).LE.TOL)GO TO 42
      WRITE(6,41)FR,DFREQ
      IF(FR.LT.FREQ) THEN
         B=B-.0001
      ELSE
         B=B+.0001
      END IF
      GOTO  40


41    FORMAT(' FREQUENCY=',F10.5,3X,'DFREQ=',F10.5)


42    WRITE(6,31)FR
31    FORMAT(' RESONANT FREQUENCY IN GIGAHERTZ=',F10.5)
      WRITE(6,32)RIN
32    FORMAT(' INPUT RESISTANCE=',F10.5)
      DFR=DFR/1.E+6/2.
      WRITE(6,33)DFR
33    FORMAT(' BANDWIDTH IN MEGAHERTZ=',F10.5)
      WRITE(6,34)EFF
34    FORMAT(' RADIATION EFFICIENCY=',F10.5)

      PERCBW=1/(Q*SQRT(2.0))
      WRITE(6,37)PERCBW
37    FORMAT(' % BW=',F10.5)
```

```
          WRITE(6,38)RCU,RDI,RAD,Q
   38     FORMAT('RCU=',F10.5,2X,'RDI=',F10.5,2X,'RAD=', F10.5,
          2X,'Q=',F10.5)
          WRITE(6,39)A,B
   39     FORMAT('WIDTH=',F10.5,5X,'LENGTH=',F10.5)

          STOP
          END
```

II.   MICARY.FOR

```
C...LINEARLY POLARIZED PLANAR ARRAY FORMED BY LINEARLY
C...POLARIZED MICROSTRIP ELEMENTS
C...WITH CROSS-POL, MODAL EXPANSION MULTIMODES ARE USED.
C...NO GTD DIFFRACTION,  ALL DIMENSIONS IN WAVELENGTHS
C...PROGRAMMED BY DR. J. HUANG AT JET PROPULSION LAB.
          DIMENSION DBR(362),DBL(182),XAX(362),XX(2),YY(2),
          1IANG(40)
          DIMENSION PHASR(182),PHASL(182),XE(40), YE(40),
          1AMP(40), PHAS(40)
          COMPLEX CJ,CJJ,EX,EY,EZ,X0,Y0,Z0,ETH,EPH,ER,EL
          COMPLEX FX,FY,FZ,X1,Y1,Z1,X2,Y2,Z2,X3,Y3,Z3
          COMMON/DD1/EPS,T,A,B,I2,IP,XS,YS,ZS,CJJ
          COMMON/DD2/CJ,PI,TPI,DPR
          COMMON/DD4/THPR,PHPR,RR

C...MODIFIED TO READ DATA FROM A GEOMETRY FILE
C...BY BILL BARFIELD, NPGS
          OPEN(33, FILE='DATA')
          OPEN(35, FILE='GEOMETRY')

          CJ=(0.,1.)
          CJJ=(1.E-15,1.E-15)
          PI=3.14159265
          TPI=2.*PI
          DPR=180./PI
          WRITE(6,1)
   1      FORMAT(' DIELECTRIC CONSTANT AND THICKNESS=?')

C         READ(5,99)EPS,T
          READ(33,*)EPS,T
          WRITE(6,99) EPS,T

  99      FORMAT( F8.6,F8.6)
  98      FORMAT(I8)
          WRITE(6,2)
   2      FORMAT(' MICROSTRIP WIDTH AND LENGTH=?')
```

63

```
C         READ(5,99)A,B
          READ(33,*)A,B
          WRITE(6,99)A,B

C...A,B ARE THE PHYSICAL WIDTHS OF THE METALLIC PATCH
C.....A ALONE X-AXIS,  B ALONE Y-AXIS, X-AXIS IS HORIZONTAL
          WRITE(6,3)
  3       FORMAT(' FIELD POINT DISTANCE AND PATTERN CUT
         /ANGLE=?')

C         READ(5,99)RF,PHD
          READ(33,*)RF,PHD
          WRITE(6,99)RF,PHD
          WRITE(6,*)RF,PHD

          WRITE(6,5)
  5       FORMAT(' FEED PROBE DIAMETER & DISTANCE FROM EDGE=?')

C         READ(5,99)D,YP
          READ(33,*)D,YP
          WRITE(6,99)D,YP

          WRITE(6,4)
  4       FORMAT(' NUMBER OF ELEMENTS=?')

C         READ(5,98)N
          READ(35,*)N
          WRITE(6,*)N

          WRITE(6,6)I
  6       FORMAT(' NUMBER',I2,2X,'X,Y LOCATION,AMPLITUDE,PHASE &
         /ORIENTATION=?')

          DO 105 I=1,N

C         READ(5,*)XW,YW,AMG,DEG,IANG(I)
          READ(35,*)XW,YW,AMG,DEG,IANG(I)
          WRITE(6,*)XW,YW,AMG,DEG,IANG(I)

          XE(I)=XW
          YE(I)=YW
          AMP(I)=AMG
          PHAS(I)=DEG/360.*TPI
  105     CONTINUE
          D=5.*D
          SK2=EPS*TPI*TPI
          PIB=(PI/B)**2
          PIA=(PI/A)**2
          F1=1./A/B/SK2
          F1=1.E-7
          CYP=COS(PI*YP/B)
```

```fortran
      F2=2./A/B/(SK2-PIB)*CYP
      SD=SIN(PI*D/A)/(PI*D/A)
      F3=4./A/B/(SK2-4.*PIA-PIB)*CYP*SD
      CYP=COS(TPI*YP/B)
      F4=4./A/B/(SK2-4.*PIA-4.*PIB)*CYP*SD
      F5=2./A/B/(SK2-4.*PIB)*CYP
      F6=2./A/B/(SK2-4.*PIA)*SD
      F7=2./A/B/(SK2-9.*PIB)*COS(3.*PI*YP/B)
C     WRITE(6,7)F1,F2,F3,F4

   7  FORMAT('F1=',F10.5,5X,'F2=',F10.5,5X,'F3=',F10.5,5X,'
     /F4=',F10.5)
C     WRITE(6,8)F5,F6,F7
   8  FORMAT(' F5=',F10.5,5X,'F6=',F10.5,5X,'F7=',F10.5)
      DO 200 I=1,181
      THDD=FLOAT(I-1)/2.-45.
      THD=ABS(THDD)
      THR=THD/DPR
      PHR=PHD/DPR
      IF(THDD.LT.0.)PHR=PHR+PI
      XS=RF*SIN(THR)*COS(PHR)
      YS=RF*SIN(THR)*SIN(PHR)
      ZS=RF*COS(THR)
      FX=CJJ
      FY=CJJ
      FZ=CJJ
      DO 104 I4=1,N
      EX=CJJ
      EY=CJJ
      EZ=CJJ
      DO 102 I2=1,4
      XA=(B+T)/2.
      IF(I2.EQ.2)XA=-XA
      IF(I2.EQ.3)XA=(A+T)/2.
      IF(I2.EQ.4)XA=-(A+T)/2.
       X=XS-XE(I4)-XA
      Y=YS-YE(I4)
      Z=ZS
      IF(I2.LT.3)X=XS-XE(I4)
      IF(I2.LT.3)Y=YS-YE(I4)-XA
      RR=SQRT(X*X+Y*Y+Z*Z)
      XU=X/RR
      YU=Y/RR
      ZU=Z/RR
      IF(ABS(XU).LT.1.E-8)XU=1.E-8
      IF(ABS(YU).LT.1.E-8)YU=1.E-8
      PHPR=ATAN2(YU,XU)
      IF(PHPR.LT.0.)PHPR=PHPR+TPI
      IF(I2.LT.3)PHPR=PHPR-PI/2.
      IF(PHPR.LT.0.)PHPR=PHPR+TPI
      THPR=ACOS(ZU)
```

```
      CALL SLOT4(X0,Y0,Z0,X1,Y1,Z1,X2,Y2,Z2,X3,Y3,Z3)
      IF(IANG(I4).EQ.270)GO TO 50
      IF(IANG(I4).EQ.90)GO TO 60
      IF(IANG(I4).EQ.180)GO TO 70
      IF(I2.EQ.2)GO TO 41
      IF(I2.EQ.3)GO TO 42
      IF(I2.EQ.4)GO TO 43
      EX=EX-(F1-F2+F5-F7)*Y0-(F4-F3+F6)*Y2
      EY=EY+(F1-F2+F5-F7)*X0+(F4-F3+F6)*X2
      EZ=EZ+(F1-F2+F5-F7)*Z0+(F4-F3+F6)*Z2
      GO TO 102
41    EX=EX+(F2+F1+F5+F7)*Y0+(F3+F4+F6)*Y2
      EY=EY-(F2+F1+F5+F7)*X0-(F3+F4+F6)*X2
      EZ=EZ-(F2+F1+F5+F7)*Z0-(F3+F4+F6)*Z2
      GO TO 102
42    EX=EX+(F1-F6)*X0+(F2-F3)*X1+(F4-F5)*X2-F7*X3
      EY=EY+(F1-F6)*Y0+(F2-F3)*Y1+(F4-F5)*Y2-F7*Y3
      EZ=EZ+(F1-F6)*Z0+(F2-F3)*Z1+(F4-F5)*Z2-F7*Z3
      GO TO 102
43    EX=EX-(F1-F6)*X0+(F3-F2)*X1-(F4-F5)*X2+F7*X3
      EY=EY-(F1-F6)*Y0+(F3-F2)*Y1-(F4-F5)*Y2+F7*Y3
      EZ=EZ-(F1-F6)*Z0+(F3-F2)*Z1-(F4-F5)*Z2+F7*Z3
      GO TO 102
50    IF(I2.EQ.2)GO TO 51
      IF(I2.EQ.3)GO TO 52
      IF(I2.EQ.4)GO TO 53
      EX=EX-((F1-F6)*Y0+(F3-F2)*Y1+(F4-F5)*Y2+F7*Y3)
      EY=EY+((F1-F6)*X0+(F3-F2)*X1+(F4-F5)*X2+F7*X3)
      EZ=EZ+((F1-F6)*Z0+(F3-F2)*Z1+(F4-F5)*Z2+F7*Z3)
      GO TO 102
51    EX=EX-(-(F1-F6)*Y0+(F2-F3)*Y1-(F4-F5)*Y2-F7*Y3)
      EY=EY+(-(F1-F6)*X0+(F2-F3)*X1-(F4-F5)*X2-F7*X3)
      EZ=EZ+(-(F1-F6)*Z0+(F2-F3)*Z1-(F4-F5)*Z2-F7*Z3)
      GO TO 102
52    EX=EX+((F1-F2+F5-F7)*X0+(F4-F3+F6)*X2)
      EY=EY+((F1-F2+F5-F7)*Y0+(F4-F3+F6)*Y2)
      EZ=EZ+((F1-F2+F5-F7)*Z0+(F4-F3+F6)*Z2)
      GO TO 102
53    EX=EX+((-F2-F1-F5-F7)*X0+(-F3-F4-F6)*X2)
      EY=EY+((-F2-F1-F5-F7)*Y0+(-F3-F4-F6)*Y2)
      EZ=EZ+((-F2-F1-F5-F7)*Z0+(-F3-F4-F6)*Z2)
      GO TO 102
60    IF(I2.EQ.2)GO TO 61
      IF(I2.EQ.3)GO TO 62
      IF(I2.EQ.4)GO TO 63
      EX=EX-((F1-F6)*Y0+(F2-F3)*Y1+(F4-F5)*Y2-F7*Y3)
      EY=EY+(F1-F6)*X0+(F2-F3)*X1+(F4-F5)*X2-F7*X3
      EZ=EZ+(F1-F6)*Z0+(F2-F3)*Z1+(F4-F5)*Z2-F7*Z3
      GO TO 102
61    EX=EX+(F1-F6)*Y0+(F2-F3)*Y1+(F4-F5)*Y2-F7*Y3
      EY=EY-((F1-F6)*X0+(F2-F3)*X1+(F4-F5)*X2-F7*X3)
```

```fortran
      EZ=EZ-((F1-F6)*Z0+(F2-F3)*Z1+(F4-F5)*Z2-F7*Z3)
      GO TO 102
62    EX=EX+(F1+F2+F5+F7)*X0+(F3+F4+F6)*X2
      EY=EY+(F1+F2+F5+F7)*Y0+(F3+F4+F6)*Y2
      EZ=EZ+(F1+F2+F5+F7)*Z0+(F3+F4+F6)*Z2
      GO TO 102
63    EX=EX+(F2-F1-F5+F7)*X0+(F3-F4-F6)*X2
      EY=EY+(F2-F1-F5+F7)*Y0+(F3-F4-F6)*Y2
      EZ=EZ+(F2-F1-F5+F7)*Z0+(F3-F4-F6)*Z2
      GO TO 102
70    IF(I2.EQ.2)GO TO 71
      IF(I2.EQ.3)GO TO 72
      IF(I2.EQ.4)GO TO 73
      EX=EX-((F1+F2+F5+F7)*Y0+(F3+F4+F6)*Y2)
      EY=EY+(F1+F2+F5+F7)*X0+(F3+F4+F6)*X2
      EZ=EZ+(F1+F2+F5+F7)*Z0+(F3+F4+F6)*Z2
      GO TO 102
71    EX=EX-((F2-F1-F5+F7)*Y0+(F3-F4-F6)*Y2)
      EY=EY+(F2-F1-F5+F7)*X0+(F3-F4-F6)*X2
      EZ=EZ+(F2-F1-F5+F7)*Z0+(F3-F4-F6)*Z2
      GO TO 102
72    EX=EX+(F1-F6)*X0+(F3-F2)*X1+(F4-F5)*X2+F7*X3
      EY=EY+(F1-F6)*Y0+(F3-F2)*Y1+(F4-F5)*Y2+F7*Y3
      EZ=EZ+(F1-F6)*Z0+(F3-F2)*Z1+(F4-F5)*Z2+F7*Z3
      GO TO 102
73    EX=EX+(F6-F1)*X0+(F2-F3)*X1+(F5-F4)*X2-F7*X3
      EY=EY+(F6-F1)*Y0+(F2-F3)*Y1+(F5-F4)*Y2-F7*Y3
      EZ=EZ+(F6-F1)*Z0+(F2-F3)*Z1+(F5-F4)*Z2-F7*Z3
102   CONTINUE
      FX=FX+EX*AMP(I4)*CEXP(-CJ*PHAS(I4))
      FY=FY+EY*AMP(I4)*CEXP(-CJ*PHAS(I4))
      FZ=FZ+EZ*AMP(I4)*CEXP(-CJ*PHAS(I4))
104   CONTINUE
      ETH=FX*COS(PHR)*COS(THR)+FY*SIN(PHR)*COS(THR)-FZ*SIN
     /(THR)
      EPH=-FX*SIN(PHR)+FY*COS(PHR)
C     ER=(ETH+CJ*EPH)/SQRT(2.)
C     EL=(ETH-CJ*EPH)/SQRT(2.)
      ER=ETH
      EL=EPH
      AER=CABS(ER)
      AEL=CABS(EL)
      IF(AER.LT.1.E-15)AER=1.E-15
      IF(AEL.LT.1.E-15)AEL=1.E-15
      IF(AER.LT.1.E-8)ER=CMPLX(1.,1.)
      IF(AEL.LT.1.E-8)EL=CMPLX(1.,1.)
      DBR(I)=20.*ALOG10(AER)
      DBL(I)=20.*ALOG10(AEL)
      PHASR(I)=ATAN2(AIMAG(ER),REAL(ER))*DPR
      PHASL(I)=ATAN2(AIMAG(EL),REAL(EL))*DPR
      XAX(I)=THDD
```

```
C         WRITE(6,*)XAX,DBR,DBL

  200    CONTINUE
         YMAXL=-1000.
         YMAXR=-1000.
         DO 22 I=1,181
         IF(YMAXR.LT.DBR(I))YMAXR=DBR(I)
         IF(YMAXL.LT.DBL(I))YMAXL=DBL(I)
  22     CONTINUE
         YMAX=YMAXR
         IF(YMAXR.LT.YMAXL)YMAX=YMAXL
         DO 21 I=1,181
         DBR(I)=DBR(I)-YMAX-2.
         DBL(I)=DBL(I)-YMAX-2.
         IF(DBR(I).LT.-40.)DBR(I)=-40.
         IF(DBL(I).LT.-40.)DBL(I)=-40.
  21     CONTINUE
C         CALL BGNPLT
C         CALL PLFORM('LINLIN',7.43,4.6)
         XX(1)=-180.
         XX(2)=180.
         YY(1)=-40.
         YY(2)=0.
C         CALL PLSCAL(XX,2,080908,YY,2,040504)
C         CALL PLGRAF('LP MICROSTRIP ARRAY','ANGLE','DB')
C         CALL PLCURV(XAX,DBR,181,0,0)
C         CALL PLNUP
C         CALL PLNTYP(5)
C         CALL PLNDN(0.,0.)
C         CALL PLCURV(XAX,DBL,181,0,0)
C         CALL ENDPLT

         J=181
         T=-181
         DO 211 I=182,362
         XAX(I)=(I-1)/2.-45.
         IF(XAX(I).GT.90.)XAX(I)=XAX(I)-180.
         DBR(I)=DBR(J)
         J=J-1
  211    CONTINUE

         OPEN(38, FILE='RESULTS.PRN')

         WRITE(6,699)
  699    FORMAT(' WRITING RESULTS TO FILE...')

  700    FORMAT(F8.3,1X,F9.3,1X)

         DO 701 I=1,361
         WRITE(38,*)XAX(I),DBR(I)
```

```fortran
701     CONTINUE

        WRITE(6,*)' DONE...'

1000    CLOSE(33)
        CLOSE(35)
        CLOSE(38)

        STOP
        END

        SUBROUTINE SLOT4(EX,EY,EZ,EX1,EY1,EZ1,EX2,
       /EY2,EZ2,EX3,EY3,EZ3)
C...RADIATION FROM DIFFERENT MODE SLOTS
        COMPLEX CJ,FAC,EPH,ETH,EX,EY,EZ,CJJ
        COMPLEX EX1,EY1,EZ1,EX2,EY2,EZ2,EX3,EY3,EZ3
        COMMON/DD1/EPS,T,AA,BB,I2,IP,XS,YS,ZS,CJJ
        COMMON/DD2/CJ,PI,TPI,DPR
        COMMON/DD4/THR,PHR,R
        FAC=CEXP(-CJ*TPI*R)/R
        A=T/2.
        B=(AA+T)/2.
        IF(I2.GT.2)B=(BB+T)/2.
        CPH=COS(PHR)
        SPH=SIN(PHR)
        CTH=COS(THR)
        STH=SIN(THR)
        ARG1=TPI*A*CPH*STH*SQRT(EPS)
        ARG2=TPI*B*SPH*STH
        IF(ABS(ARG1).LT.1.E-4)GO TO 11
        F1=SIN(ARG1)/ARG1
        GO TO 12
11      F1=1.
12      IF(ABS(ARG2).LT.1.E-4)GO TO 13
        F2=SIN(ARG2)/ARG2
        GO TO 14
13      F2=1.
14      IF(ABS(ABS(ARG2)-PI/2.).LT.1.E-4)GO TO 15
        F3=ARG2*COS(ARG2)/(ARG2*ARG2-PI*PI/4.)
        GO TO 16
15      F3=-1./PI*ARG2
16      F4=COS(ARG2)/(ARG2*ARG2-PI*PI)
        IF(ABS(ABS(ARG2)-1.5*PI).LT.1.E-4)GO TO 17
        F5=ARG2*COS(ARG2)/(ARG2*ARG2-PI*PI*9./4.)
        GO TO 18
17      F5=-1./2.
18      EPH=-CJ*F1*F2*SPH*CTH*FAC
        ETH=CJ*F1*F2*CPH*FAC
        EX=ETH*CTH*CPH-EPH*SPH
        EY=ETH*CTH*SPH+EPH*CPH
        EZ=-ETH*STH
```

```fortran
      EPH=-F1*F3*SPH*CTH*FAC
      ETH=F1*F3*CPH*FAC
      EX1=ETH*CTH*CPH-EPH*SPH
      EY1=ETH*CTH*SPH+EPH*CPH
      EZ1=-ETH*STH
      EPH=CJ*PI*F1*F4*SPH*CTH*FAC
      ETH=-CJ*PI*F1*F4*CPH*FAC
      EX2=ETH*CTH*CPH-EPH*SPH
      EY2=ETH*CTH*SPH+EPH*CPH
      EZ2=-ETH*STH
      EPH=F1*F5*SPH*CTH*FAC
      ETH=-F1*F5*CPH*FAC
      EX3=ETH*CTH*CPH-EPH*SPH
      EY3=ETH*CTH*SPH+EPH*CPH
      EZ3=-ETH*STH
      RETURN
       END
```

III. GEOM.FOR

```fortran
C...ROUTINE TO CREATE GEOMETRY FOR MICARY.FOR
      DIMENSION X(4),Y(9),SMAGD(9,4),SPHASED(9,4)
      REAL L,W,AMP,PHASE,LAMBDA,FREQ,SPACE

      OPEN(5,FILE='GEOMETRY')
       OPEN(33,FILE='MAG')
       OPEN(35,FILE='PHASE')

C...READ IN MAGNITUDE AND PHASE DATA FROM FILE

      NUMX=4
      NUMY=9
      NUMTOT=NUMX*NUMY

      DO  4 I=1,NUMY
      READ(33,*)SMAGD(I,1),SMAGD(I,2),SMAGD(I,3),SMAGD(I,4)
      READ(35,*)SPHASED(I,1),SPHASED(I,2),SPHASED(I,3),
     /SPHASED (I,4)
      WRITE(6,*)SMAGD(I,1),SMAGD(I,2),SMAGD(I,3),SMAGD(I,4)
      WRITE(6,*)SPHASED(I,1),SPHASED(I,2),SPHASED(I,3),
     /SPHASED (I,4)

  4    CONTINUE

  12   FORMAT(F10.5,F10.5,F10.5,F10.5)

C...FREQUENCY IN HZ
      FREQ=1618.25E6
      LAMBDA=3.E8/FREQ
```

```
C...DIMENSIONS IN CM
      L=4.44
      W=5.9
      AMP=1.0
      PHASE=.0
      ORIENT=0.
      SPACE=.55*LAMBDA

C...CONVERT TO WAVELENGTHS
      L=L/100.
      L=L/LAMBDA
      W=W/100.
      W=W/LAMBDA

      DO 10 I=1,NUMX
      X(I)=(I-1)*SPACE+(I-1)*W
 10   CONTINUE

      DO 15 I=1,NUMY
      Y(I)=(I-1)*SPACE+(I-1)*L
 15   CONTINUE

      NUMEL=NUMX*NUMY
      WRITE(5,98)NUMEL
 98   FORMAT(I3)

       K=0
       N=0
       ORIENT=0
       DO 20 I=1,9
       DO 22 J=1,4

        K=K+1

      WRITE(5,99)X(J),Y(I),SMAGD(I,J),SPHASED(I,J),N

 22   CONTINUE
 20   CONTINUE

 99   FORMAT(F8.3,1X,F8.3,1X,F8.3,1X,F8.3,1X,I1)

      STOP
      END
```
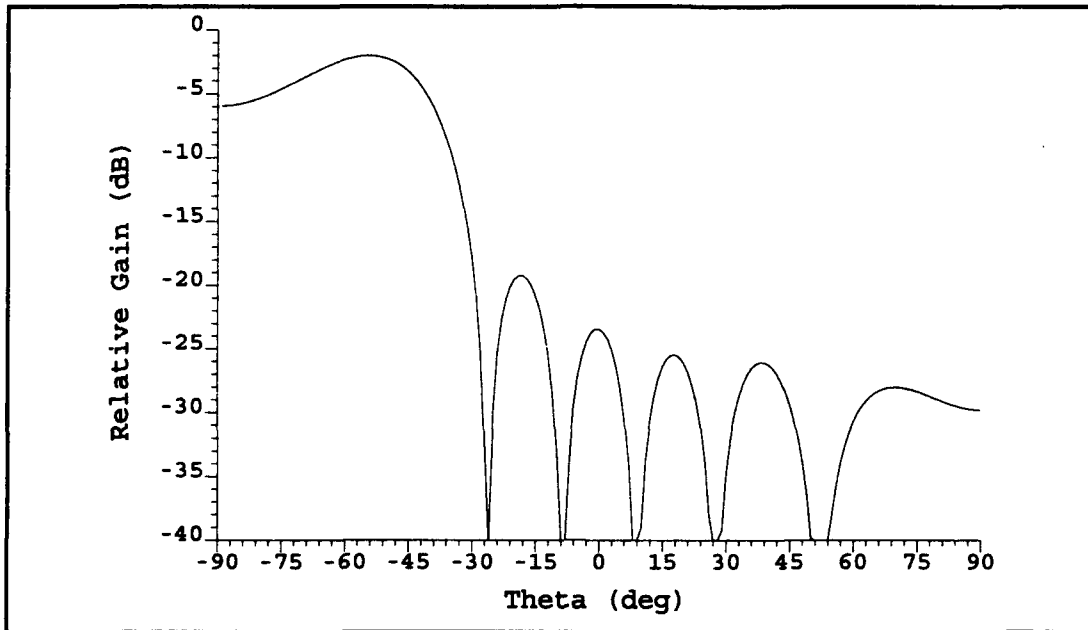
APPENDIX G

I. RADIATION PATTERNS

Figure G-1. Beam 1 Radiation pattern (φ=90°)
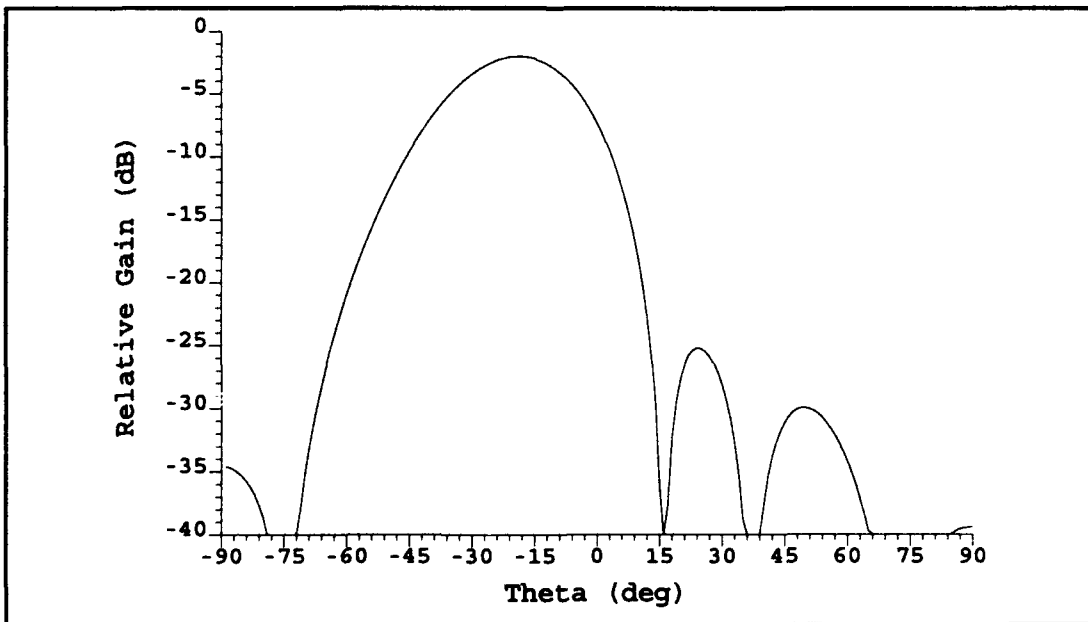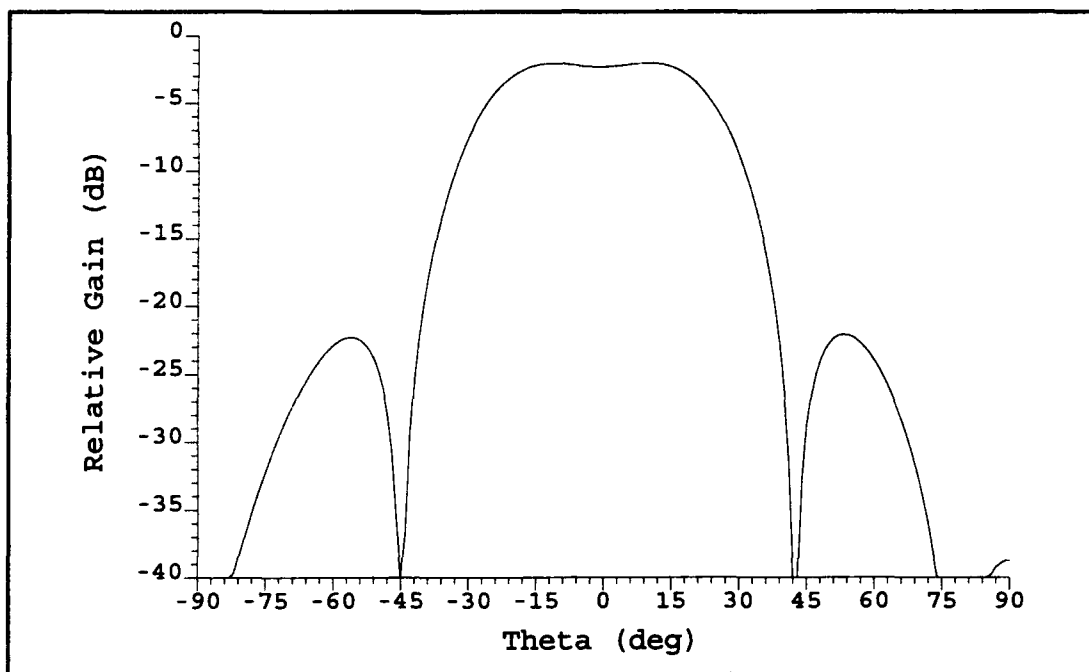

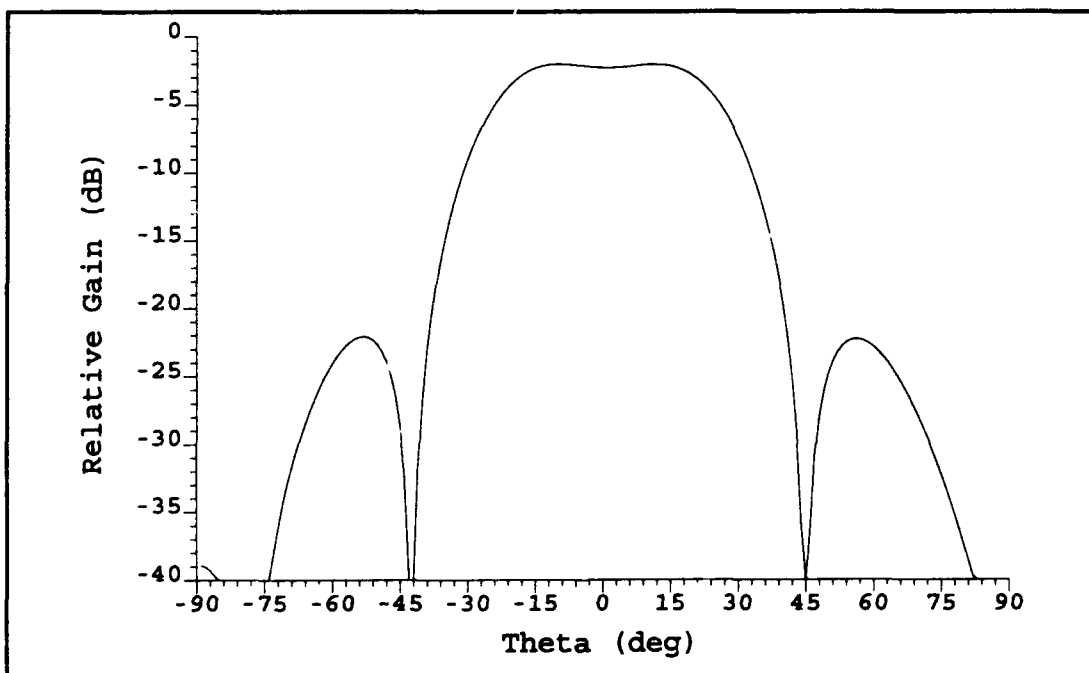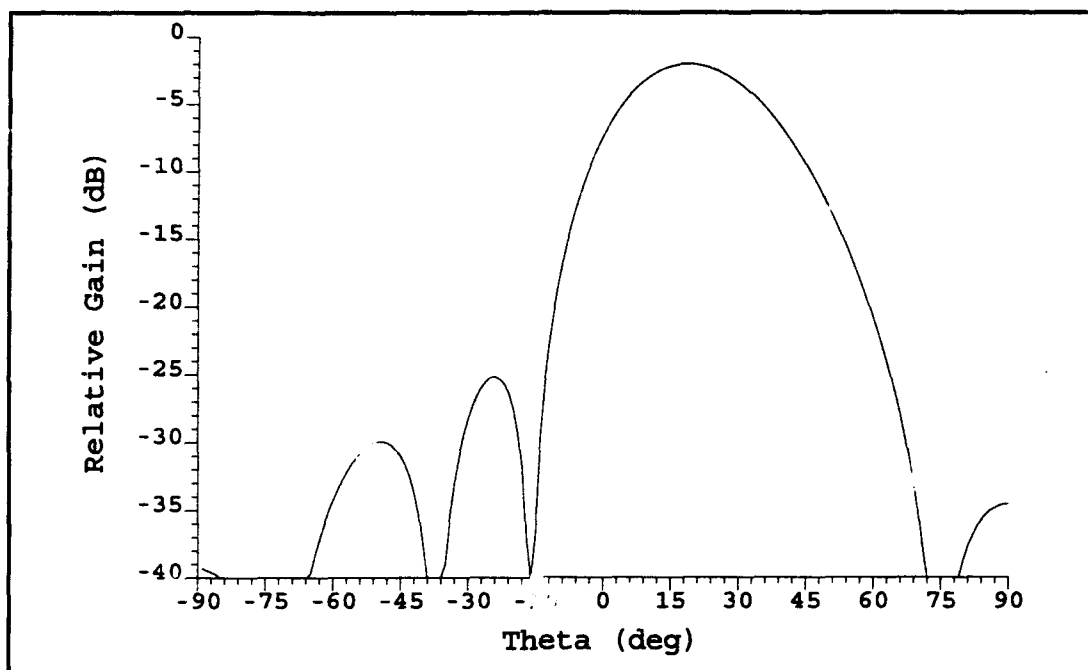**Figure G-2. Beam 2 Radiation Pattern (φ=90°)**

Figure G-3. Beam 3 Radiation Pattern (φ=90°)

Figure G-4. Beam 4 Radiation Pattern (φ=90°)

Figure G-5. Beam 5 Radiation Pattern (φ=90°)
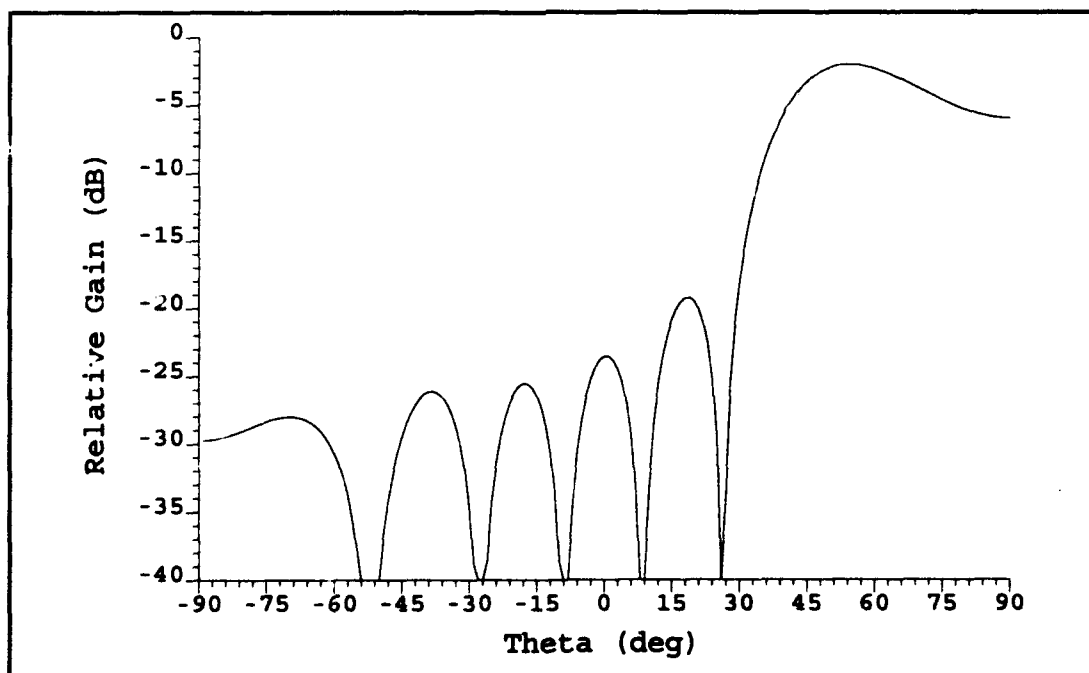
Figure G-6. Beam 6 Radiation Pattern (φ=90°)

74

II.   PATTERN SEPARATION
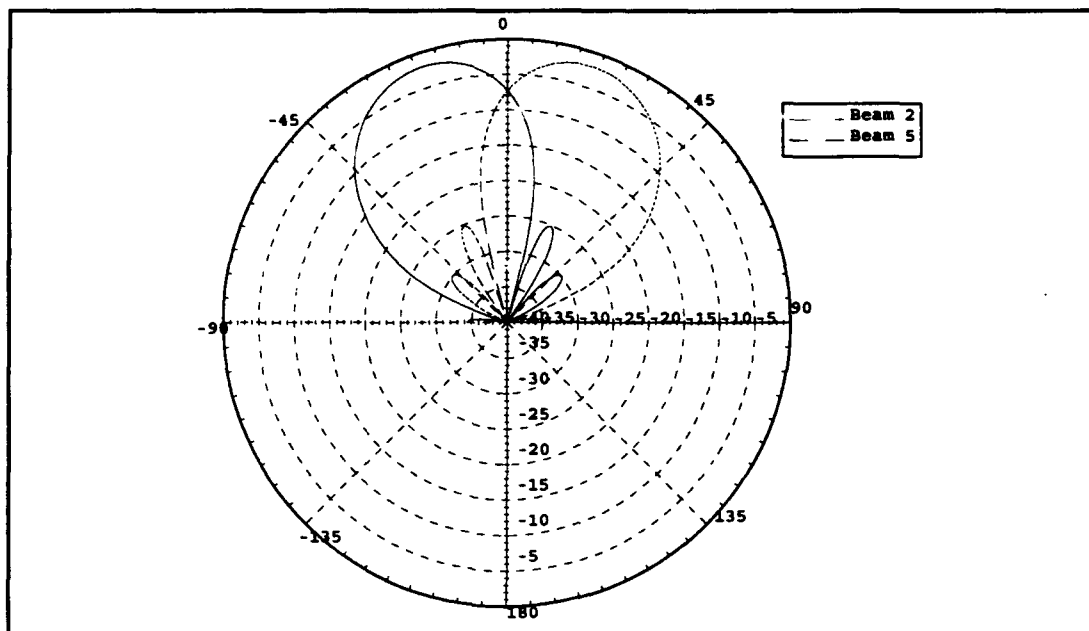
Figure G-7.   Simultaneous Radiation
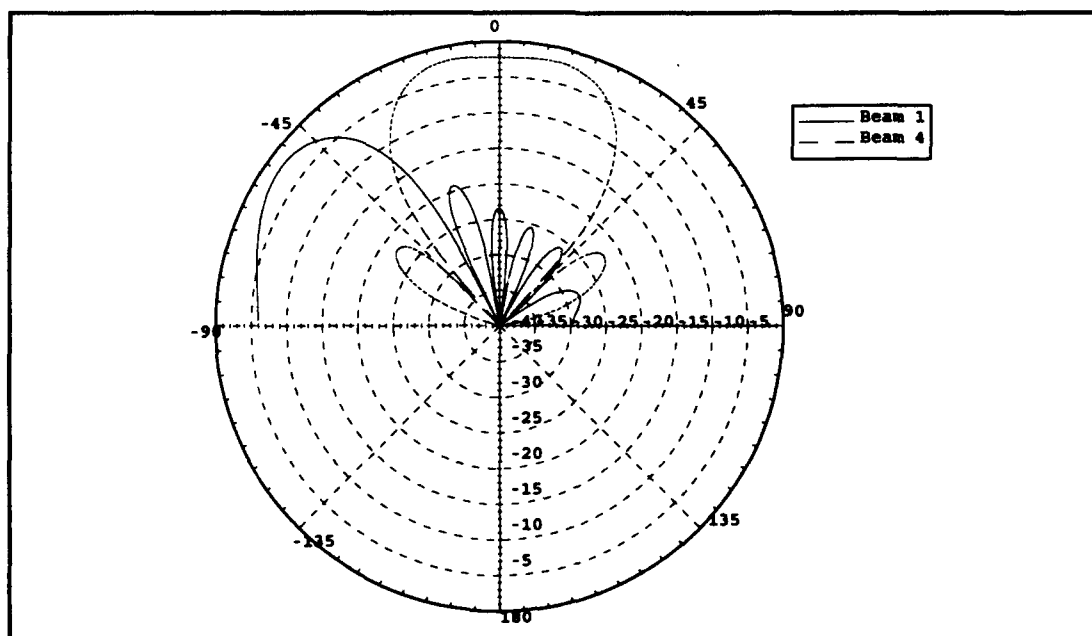
Figure G-8.   Simultaneous Radiation
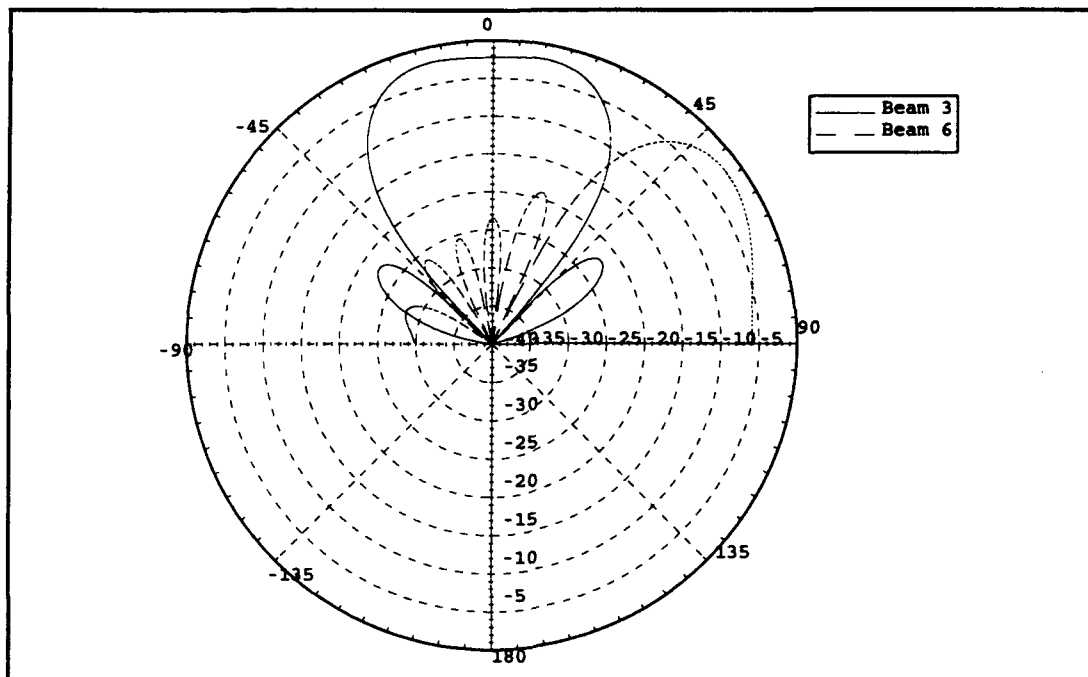
Figure G-9. Simultaneous Radiation

III. ANTENNA FOOTPRINT

Figure G-10. Beam 1 Relative dB Gain Footprint

Relative dB Contours
(Beam scanned 27 degrees from nadir)

Figure G-11. Beam 2 Relative dB Gain Footprint

Relative dB Contours
(Beam scanned 10 degrees left of nadir)
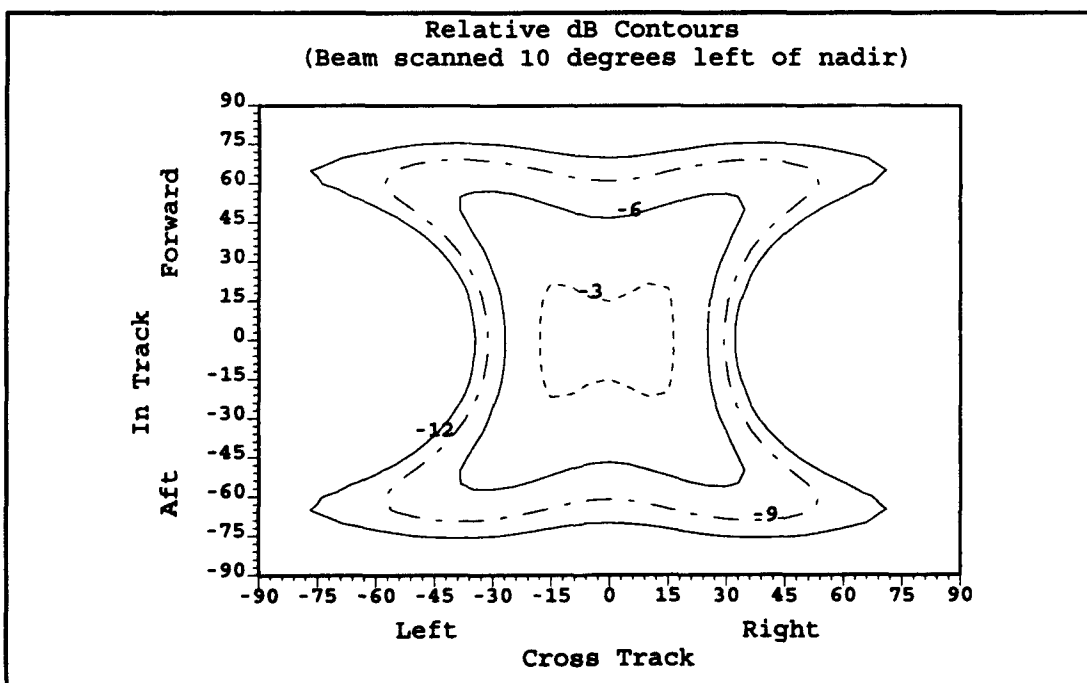
Figure G-12. Beam 3 Relative dB Gain Footprint

Relative dB Contours
(Beam scanned 10 degrees right of nadir)
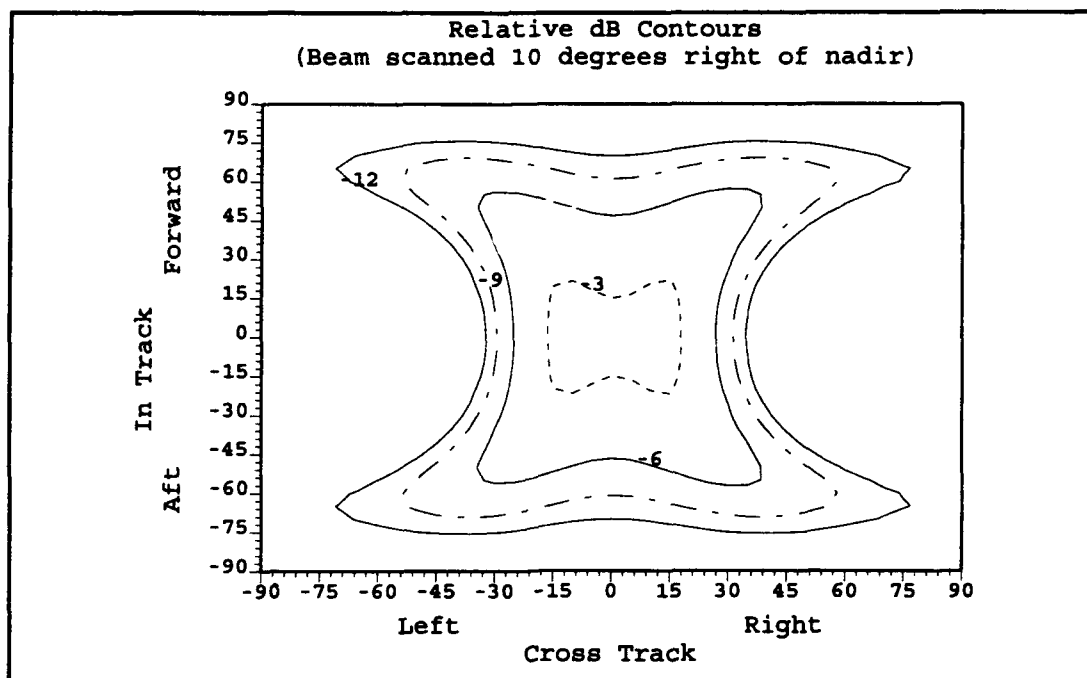
Figure G-13. Beam 4 Relative dB Gain Footprint

Relative dB Contours
(Beam scanned 27 degrees from nadir)
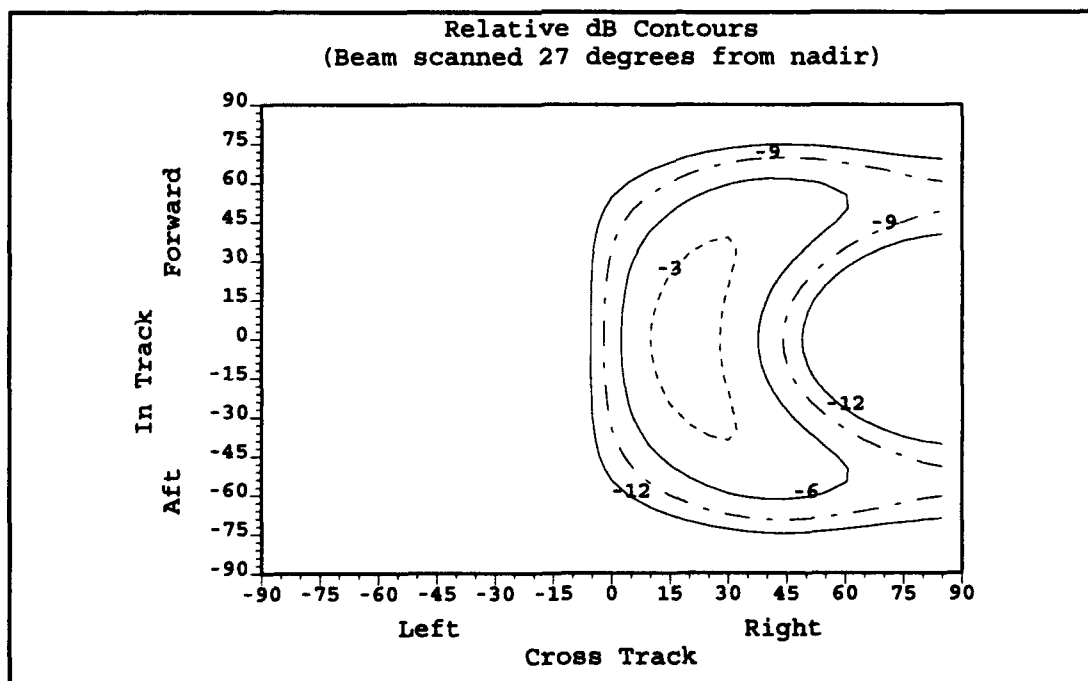
Figure G-14. Beam 5 Relative dB Gain Footprint
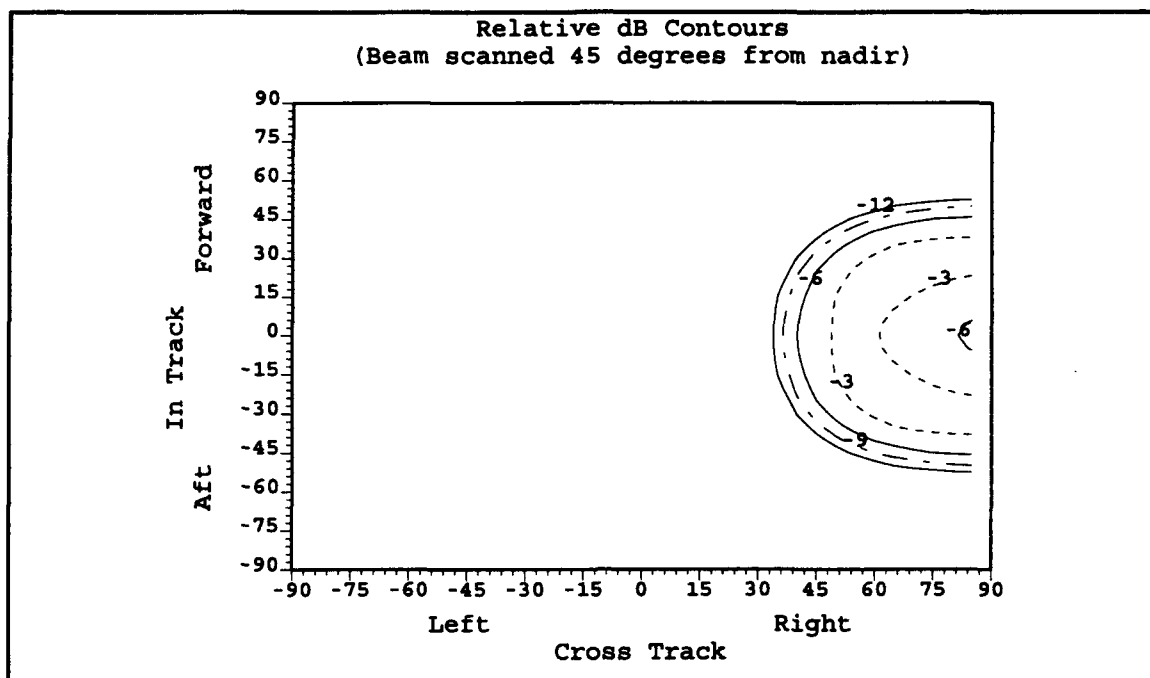
Figure G-15. Beam 6 Relative dB Gain Footprint

LIST OF REFERENCES

1. LORAL Cellular Systems, Corp. Application of Loral Cellular Systems, Before the Federal Communications Commission, Washington, D.C., June 3, 1991.

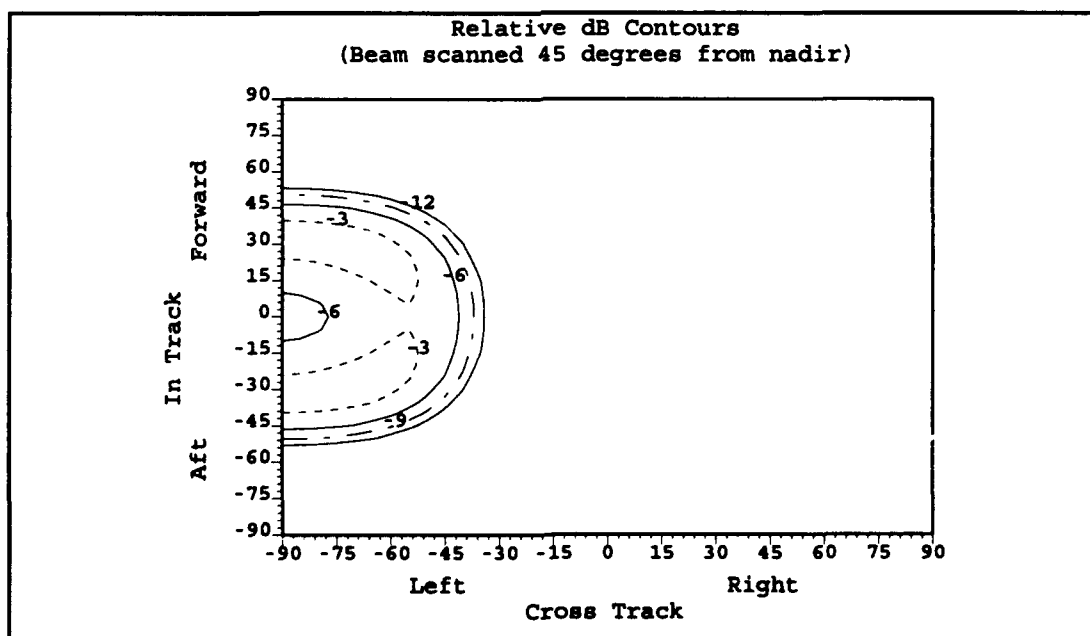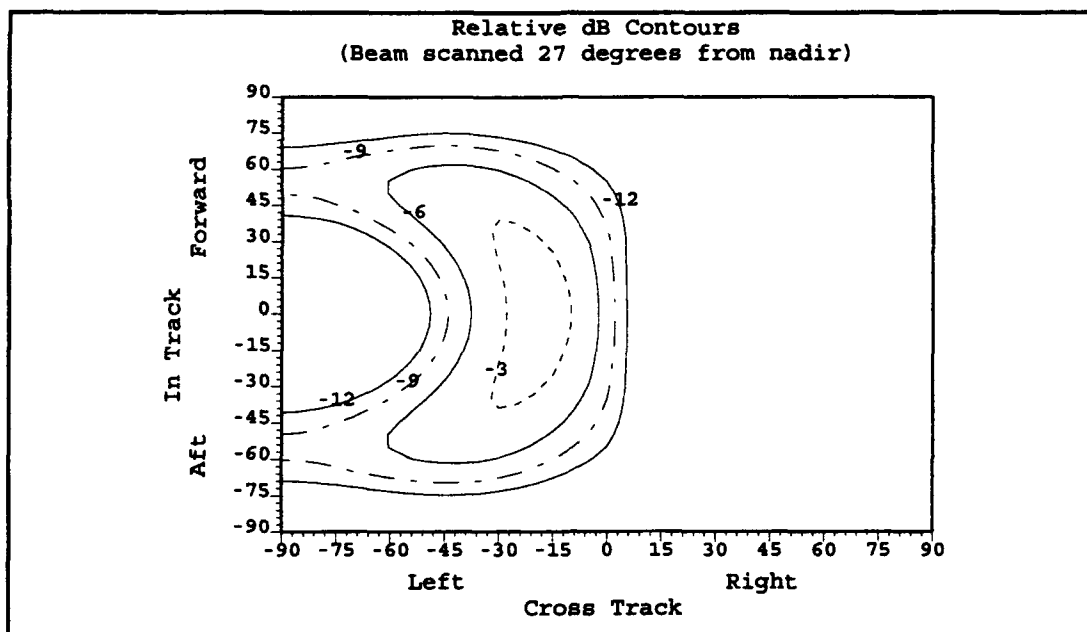2. Agrawal, Brij N., Ph.D., Spacecraft Design Project: Low Earth Orbit Communications Satellite, Naval Postgraduate School, Monterey, CA, December, 1991.

3. Huang, John, Microstrip Antenna Developments at JPL, IEEE Antennas and Propagation Magazine, V. 33. No. 3., pp. 33-41, June, 1991.

4. Mailloux, Robert, J., McIlvenna, John, F., and Kernweis, Nichols, P., Microstrip Array Technology, IEEE Transactions Antennas and Propagation, V. AP-29, No. 1, pp. 25-35, January, 1981.

5. Carver, Keith, R., and Mink, James, W., Microstrip Antenna Technology, IEEE Transactions Antenna and Propagation, V. AP-29, No. 1, pp. 1-24, January, 1981.

6. Bahl, I. J., and Bhartia, P. Microstrip Antennas, Artech House, Inc., Norwood, MA, 1980.

7. Richards, William, F., Lo, Yuen, T., and Harrison, Daniel, D., An Improved Theory for Microstrip Antennas and Applications, IEEE Transactions Antennas and Propagation, V. AP-29, No. 1, pp. 38-46, January, 1981.

8. Balanis, Constantine, A., Antenna Theory, Analysis and Design, John Wiley & Sons, New York, NY, 1982.

9. Guy, R.F.E., General Radiation Pattern Synthesis Techniques for Array Antennas of Arbitrary Configuration and Element Type, IEE Proceedings, Pt. H., V. 135, No. 4, pp. 241-248, August, 1988.

10. Ng, Tung, Sang, Generalized Array Pattern Synthesis Using the Projection Matrix, IEE Proceedings, V. 132, Pt. H, No. 1, pp. 44-46 February, 1985.

11. Bucci, O. M., Franceschetti, G., Mazzarella, G., and Panariello, G., _Intersection Approach to Array Pattern Synthesis_, IEE Proceedings, V., 137, Pt. H, No. 6, pp. 349-357, December, 1990.

12. Pozar, David, M., _General Relations for a Phased Array of Printed Antennas Derived from Infinite Current Sheets_, IEEE Transactions Antennas and Propagation, V. AP-33, No. 5, pp. 498-504, May, 1985.

13. Splitt, Georg, and Davidovitz, Marat, _Guidelines for Design of Electromagnetically Coupled Microstrip Patch Antennas on Two-Layer Substrates_, IEEE Transactions Antennas and Propagation, V. 38, No. 7, pp. 1136-1140, July, 1990.

14. Pozar, David, M., and Kaufman, Barry, _Design Considerations for Low Sidelobe Microstrip Arrays_, IEEE Transactions Antennas and Propagation, V. 38, No. 8, pp. 1176-1185, August, 1990.

15. Jedlicka, R.P., Poe, M. T., and Carver, K. R., _Measured Mutual Coupling Between Microstrip Antennas_, IEEE Transactions Antennas and Propagation, V. AP-29, No. 1, pp. 147-149, January, 1981.

16. Pozar, David, M., _Input Impedance and Mutual Coupling of Rectangular Microstrip Antennas_, IEEE Transactions Antennas and Propagation, V. AP-30, No. 6, pp. 1193-1196, November, 1982.

17. Navarro, Julio, A., Hummer, Kenneth, A., and Chang, Kai, _Active Integrated Antenna Elements_, Microwave Journal, pp. 115-126, January, 1991.

18. Thomas, H. J., Fudge, D. L., and Morris, G., _Gunn Source Integrated with Microstrip Patch_, Microwaves and RF, pp. 87-91, February, 1985.

19. James, J. R., Hall, P. S., and Wood, C., _Microstrip Antenna Theory and Design_, Peter Peregrinus LTD., Piscataway, NJ, 1981.

20. Hall, P. S., and James, J. R., _Design of Microstrip Antenna Feeds Pt. I and II_, IEE Proceedings, V. 128, Pt. H, No. 1, pp. 19-36, February, 1981.

21. Pozar, David, M., _Finite Phased Arrays of Rectangular Microstrip Patches_, IEEE Transactions Antennas and Propagation, V. AP-34, No. 5, pp. 658-665, May, 1986.

22.   Huang, John, <u>The Finite Ground Plane Effect on the
       Microstrip Antenna Radiation Patterns</u>, IEEE
       Transactions Antennas and Propagation, V. AP-31, No.
       4, pp. 649-653, July, 1983.

23.   Aberle, J. T., and Pozar, D. M., <u>Analysis of Infinite
       Arrays of Probe-Fed Rectangular Microstrip Patches
       Using a Rigorous Feed Model</u>, IEE Proceedings, Pt. H,
       V. 136, No. 2, pp. 110-119, April, 1989.

24.   Newman, Edward H., and Tulyathan, Pravit, <u>Analysis of
       Microstrip Antennas Using Moment Methods</u>, IEEE
       Transac-tions Antennas and Propagation, V. AP-29, No.
       1, pp. 47-52, January, 1981.

25.   Yang, Hung-Yu, Nakatani, Akifumi, and Castaneda,
       Jesse, A., <u>Efficient Evaluation of Spectral Integrals
       in the Moment Method Solution of Microstrip Antennas
       and Circuits</u>, IEEE Transactions Antennas and
       Propagation, V. 38, No. 7, pp. 1127-1129, July, 1990.

26.   Bokhari, S. A., Mosig, J. R., and Gardiol, F. E.,
       <u>Hybrid Approach to Compute Radiation Pattern of Finite
       Micro-strip Antennas</u>, Electronics Letters, V. 27, No.
       22, pp. 2091-2093, October, 1991.

27.   Hall, P., S., and Vetterlein, S. J., <u>Integrated
       Multiple Beam Microstrip Arrays</u>, Microwave Journal,
       pp. 103-114, January, 1992.

28.   Hall, P. S., and Vetterlein, S. J., <u>Multiple Beam
       Micro-strip Patch Array With Integrated Beamformer</u>,
       IEE Proceedings, Pt. H, V. 138, No. 2, pp. 176-184,
       April, 1991.

BIBLIOGRAPHY

Abboud, F., Damiano, J.P., and Papiernik, A., *Simple Model for the Input Impedance of Coax-Fed Rectangular Microstrip Patch Antenna for CAD*, IEE Proceedings, Pt. H, V. 135, No. 5, October, 1985.

An, H., Nauwelaers, B., and Van De Capelle, A., *Matching Network Design of Microstrip Antennas with Simplified Real Frequency Technique*, Electronics Letters, V. 27, No. 24, November, 1991.

Brennan, P.V., *Low Cost Phased Array Antenna for Land-Mobile Satcom Applications*, IEE Proceedings, Pt. H, V. 138, No. 2, April, 1991.

Couch, Leon, W., *Digital and Analog Communications Systems*, Macmillan, New York, NY, 1990.

Franceschetti, G., Mazzarella G., and Panariello, G., *Array Synthesis with Excitation Constraints*, IEE Proceedings, Pt. H, V. 135, No. 6, December, 1988.

Gagliardi, Robert, M., *Satellite Communications*, Van Nostrand Reinhold, New York, NY, 1991.

Ha, Tri, T., *Digital Satellite Communications*, McGraw-Hill, New York, NY, 1990.

Hall, R.C. and Mosig, J.R., *Rigorous Feed Model for Coaxially Fed Microstrip Antenna*, Electronics Letters, V. 26, No. 1, January, 1990.

Hall, P.S., and Vetterlein, S.J., *Integrated Multiple Beam Microstrip Arrays*, Microwave Journal, January, 1992.

Henderson, A. and James, J.R., *Design of Microstrip Antenna Feeds Part I and II*, IEE Proceedings, Pt. H, V. 128, No. 1, February, 1981.

Kang, Yoon-Won and Pozar, David, M., *Correction of Error in Reduced Sidelobe Synthesis due to Mutual Coupling*, IEEE Transactions Antennas and Propagation, V. AP-33, No. 9, September, 1985.

McNamara, D.A. and Botha, E., *Transformation-Based Synthesis Technique for Planar Arrays with Contoured Beams*, Electronics Letters, V. 27, No. 17, August, 1991.

Orchard, H.J., *Optimizing the Synthesis of Shaped Beam Antenna Patterns*, IEE Proceedings, Pt. H, V. 132, No. 1, February, 1985.

Parini, C.G., Brian, D., Kalatizadeh, Y., Olver, A.D., and Raghavan, K., *Design Aspects and Tolerances in Array Fed Contour Beam Antennas of INTELSAT VI Type*, IEE Proceedings, Pt. H, V. 135, No. 6, December. 1988.

Patel, P.D. and Chan, K.K., *Optimization of Contoured Beams for Satellite Antennas*, IEE Proceedings, Pt. H, V. 132, October, 1985.

Pozar, David, M., *Microwave Engineering*, Addison-Wesley, Reading, MA, 1990.

Tonye, E. and Ngaku, J., *Green's Function Based Digital Technique Applied to the Analysis of an Antenna Consisting of a Network of Microstrip Patches*, International Journal of Electronics, V. 69, No. 4, 1990.

INITIAL DISTRIBUTION LIST

1. Defense Technical Information Center   2
   Cameron Station
   Alexandria, VA 22304-6145

2. Library, Code 52   2
   Naval Postgraduate School
   Monterey, CA 93943-5101

3. Chairman, Code EC   1
   Department of Electrical and Computer Engineering
   Naval Postgraduate School
   Monterey, CA 93943-5121

4. R. W. Adler, Code EC/Ab   2
   Department of Electrical and Computer Engineering
   Naval Postgraduate School
   Monterey, CA 93943-5121

5. Rudy Panholzer, Code EC/Pz   1
   Department of Electrical and Computer Engineering
   Naval Postgraduate School
   Monterey, CA 93943-5121

6. LT James A. Frank   1
   8508 Blue Bird Woods Ct.
   Lorton, VA 22079

7. LCDR Randall Butler   1
   PSC 477 Box 417
   FPO AP 96306-1299

8. LT Stephanie Kessler   1
   COMUSNAVCENT Code N2
   FPO AE 09501-6009

9. LT William L. Barfield   2
   2836 Kelly Square
   Vienna, VA 22181